Cell. Mol. Life Sci. (2011) 68:2281–2301
DOI 10.1007/s00018-011-0719-1

Cellular and Molecular Life Sciences

MULTI-AUTHOR REVIEW

Fluorescence spectroscopy and molecular dynamics simulations in studies on the mechanism of membrane destabilization by antimicrobial peptides

Gianfranco Bocchinfuso · Sara Bobone · Claudia Mazzuca · Antonio Palleschi · Lorenzo Stella

Received: 19 April 2011 / Revised: 26 April 2011 / Accepted: 26 April 2011 / Published online: 17 May 2011

Abstract Since their initial discovery, 30 years ago, antimicrobial peptides (AMPs) have been intensely investigated as a possible solution to the increasing problem of drug-resistant bacteria. The interaction of antimicrobial peptides with the cellular membrane of bacteria is the key step of their mechanism of action. Fluorescence spectroscopy can provide several structural details on peptide–membrane systems, such as partition free energy, aggregation state, peptide position and orientation in the bilayer, and the effects of the peptides on the membrane order. However, these "low-resolution" structural data are hardly sufficient to define the structural requirements for the pore formation process. Molecular dynamics simulations, on the other hand, provide atomic-level information on the structure and dynamics of the peptide–membrane system, but they need to be validated experimentally. In this review we summarize the information that can be obtained by both approaches, highlighting their versatility and complementarity, suggesting that their synergistic application could lead to a new level of insight into the mechanism of membrane destabilization by AMPs.

Keywords Fluorescence · Molecular dynamics · FRET · Anisotropy · Lifetimes · Excimers · Coarse graining · Potential of mean force

G. Bocchinfuso · S. Bobone · C. Mazzuca · A. Palleschi · L. Stella (✉)
Dipartimento di Scienze e Tecnologie Chimiche, Università di Roma Tor Vergata, Via della Ricerca Scientifica 1, 00133 Rome, Italy
e-mail: stella@stc.uniroma2.it

A. Palleschi · L. Stella
IRCCS Neuromed, 86077 Pozzilli, IS, Italy

Abbreviations

AA	All-atoms
AMP	Antimicrobial peptide
ANTS	Disodium 8-amino-1,3,6-naphthalenetrisulfonate
BSA	Bovine serum albumin
C6-NBD-PC	1-Palmitoyl-2-{6-[(7-nitro-2-1,3-benzoxadiazol-4-yl)amino]hexanoyl}-*sn*-glycero-3-phosphocholine
CG	Coarse-grained
Dansyl	5-(Dimethylamino)naphthalene-1-sulfonyl
DDQ	Depth-dependent quenching
DPA	Dipicolinic acid
DPH	1,6-Diphenyl-1,3,5-hexatriene
DPX	*p*-Xylene-bis(*N*-pyridinium bromide)
FCS	Fluorescence correlation spectroscopy
FRAP	Fluorescence recovery after photobleaching
FRET	Förster resonance energy transfer
GUV	Giant unilamellar vesicle
KBFI	Potassium-binding benzofuran isophthalate
Laurdan	6-Dodecanoyl-*N*,*N*-dimethyl-2-naphthylamine
LUV	Large unilamellar vesicle
MD	Molecular dynamics
NBD	7-Nitro-2-1,3-benzoxadiazol-4-yl
PC	Phosphatidylcholine
PE	Phosphatidylethanolamine
PG	Phosphatidylglycerol
PMF	Potential of mean force
SBFI	Sodium-binding benzofuran isophthalate
SUV	Small unilamellar vesicle
Trp	Tryptophan
Tyr	Tyrosine

Introduction

Antimicrobial peptides (AMPs) constitute an important component of the innate defense of all organisms [1]. They have multiple functions, including antiseptic, chemotactic, and immunomodulatory roles [2], but their main activity is bactericidal, and it is mediated by their interaction with the cellular membrane of pathogens and perturbation of its permeability [3]. When AMPs were first isolated, it was immediately evident that they induce rapid lysis of bacterial cells, even though the possibility that this was a secondary effect could not be ruled out [4]. However, it was soon observed that synthetic enantiomers of the natural peptides usually exhibit the same antimicrobial activity as the parent molecules [5], and membrane perturbation was demonstrated also in model bilayers composed of phospholipids only [6]. Therefore, no chiral interaction with other biomacromolecules is involved in the mechanism of action of most AMPs, and their ability to induce membrane leakage can be explained simply on the basis of their physical interaction with the phospholipid bilayer. Indeed, recently, Melo and co-workers [7] showed that membrane leakage takes place in bacteria and in artificial vesicles at the same membrane-bound peptide to lipid ratio. Although the correlation between results found in bacteria and in model membranes is not general, all these findings point to the fact that peptide–membrane interaction is a key factor in the mechanism of action of AMPs.

As a consequence of their target, development of bacterial resistance to AMPs is much less likely than for traditional antibiotics [8]. For this reason, these peptides are promising lead compounds for the development of a new class of antibiotic drugs [9], to address the growing problem of pathogenic organisms that have multiple resistance to traditional antimicrobial agents.

However, peptides present several limitations to their direct clinical application, such as high production costs and susceptibility to proteolytic degradation [9]. A detailed understanding of the molecular details of the membrane permeabilization process would allow the rational design of new molecules with the same mechanism of action, but with improved activity, selectivity, and bioavailability. However, even after many years, a molecular understanding of the mechanism of membrane perturbation by AMPs is still lacking [10, 11].

One of the first models proposed for the membrane permeabilization process was the formation of "barrel-stave" channels [12, 13]. According to this mechanism, peptides aggregate in a transbilayer orientation, with their apolar residues pointing towards the hydrophobic core of the membrane, and their hydrophilic faces lining a water-filled pore, reminiscent of a membrane protein ion channel. After more than 30 years, a barrel-stave channel has been demonstrated conclusively essentially only for the peptaibol alamethicin. The Shai, Matsuzaki, and Huang model [14–16] involves the accumulation of AMPs on the membrane surface. When a threshold peptide/lipid ratio is reached, the strain caused by peptide insertion in the head groups region of the membrane is released by the formation of defects, which cause leakage. Within this general framework, different variations of the model exist: Huang and co-workers [16], on the basis of neutron scattering and other biophysical data, proposed the existence of pores with a well-defined toroidal structure, in which the membrane bends back onto itself in a doughnut shape, with the peptides interspersed between phospholipid heads ("toroidal pore" model). More recently, Marrink and co-workers [17, 18] proposed a more disordered pore structure, essentially similar to a peptide-induced defect, based on the results of molecular dynamics simulations ("disordered toroidal pore" model). Bechinger and Lohner [3, 19] proposed that the action of the amphiphilic AMPs is essentially similar to that of detergents ("detergent" model). Our group [20] and Wimley [10] pointed out that some local disorder can be caused by peptides with an imperfect amphiphilic arrangement of their side-chains, by inserting some charged groups in the hydrophobic core of the membrane, thus drawing some lipid polar heads and water molecules inside the bilayer ("interfacial activity" model). Other hypotheses have been put forward, including the "sinking raft" model [21], in which several peptides form an aggregate, which can diffuse through the membrane, or the "leaky slit" model [22], in which the peptides are oriented perpendicularly to the membrane, but, rather than forming a circular pore, they aggregate side by side to form an amphipathic ribbon. The hydrophobic face of the ribbon is oriented towards the hydrocarbon chains of the bilayer, while toxicity is caused by the hydrophilic face, as this side of the ribbon cannot seal with the opposing contacting bilayer by hydrophobic interactions. As a consequence, lipids are forced to adopt a highly positive curvature, causing the membrane to bend onto itself. Another possible mechanism of membrane destabilization was recently proposed by Epand [23]: cationic AMPs could cause clustering of anionic lipids and domain formation. Phase boundaries between domains could lead to membrane leakage ("lipid clustering" model), or the perturbed lateral structure of the membrane could disrupt essential processes in the bacterial cell, such as the function of membrane proteins or specific protein–protein interactions ("sand in a gearbox" model) [24].

This plethora of models stresses the complexity of the problem. In some cases, different mechanisms have been proposed to apply for the same peptide, depending on the specific techniques and experimental conditions used to investigate them [25]. The main reason for this lack of

clarity on the mechanism of membrane destabilization by AMPs is due mainly to the difficulties involved in the application of atomic-resolution structural techniques (X-ray crystallography and NMR spectroscopy) to peptide–membrane systems. Although significant advances are being achieved in these areas [13, 26] determination of the structure of peptides and proteins in membranes is still a challenge [27], and the experimental conditions needed by these techniques often deviate from the physiological ones. For this reason, alternative approaches are particularly useful in this field.

Fluorescence spectroscopy can be easily applied to model membrane systems, and even to live cells. It presents the advantages of extreme sensitivity, minimal perturbation, and an intrinsic timescale suitable to follow the dynamic processes that take place in a lipid bilayer. It can provide a wealth of information on peptide–membrane interactions, such as the affinity of the peptide for the membrane phase, its location and orientation in the bilayer, its aggregation state, and its effects on membrane structure and integrity. However, these low-resolution structural data are hardly sufficient for a clear structural interpretation of the pore formation mechanism. On the other hand, molecular dynamics (MD) simulations provide atomic-level data on the structure and dynamics of peptide–membrane systems, but they require validation by comparisons with experimental results. Since the first discovery of AMPs, fluorescence has always been one of the main experimental approaches employed in their characterization, and in recent years MD simulation of complex peptide–membrane systems became feasible thanks to the increases in available computational power. However, only a few studies [20, 28] realized the potential of a combined application of these two approaches. In this review we summarize the main structural information that can be obtained on AMPs by both methods, with the aim to highlight their versatility and complementarity, and the advantages of a synergistic application of these two techniques in the characterization of the membrane destabilization process.

Several good reviews have been published over the years on specific topics regarding the application of fluorescence methods [29–46] and MD simulations [47–54] to studies of peptide–membrane interactions. The reader is referred to them, and to the original publications, for additional details that could not be included here because of space limitations. For the same reasons, this review cannot be exhaustive; for instance it does not discuss fluorescence correlation spectroscopy (FCS) [55, 56], fluorescence recovery after photobleaching (FRAP) [57], and fluorescence approaches to study the electrostatic properties of membranes [44].

A primer on fluorescence and MD methods

Here we wish to give a very brief introduction to the physical principles and techniques on which the experiments and simulations described in the following sections are based.

Fluorescence

Molecular fluorescence is the emission of light from a molecule (fluorophore) which was previously brought to its excited state by the absorption of a photon [58]. In addition to light emission, the excited molecule can release its excess energy by other nonradiative processes, transferring it to the environment, and these phenomena compete with fluorescence. Therefore, the intensity of emitted light and the lifetime of the excited state depend strongly on the fluorophore's environment. As a result of interactions between the probe and the surrounding molecules, the wavelength of emitted light is also strongly dependent on the probe's environment.

The main experimental advantage of fluorescence is its extreme sensitivity. With today's instrumentation it is easy to perform experiments with micro- to nanomolar concentrations, and it is possible to measure light emission even from single molecules. Additionally, the lifetime of the excited state (typically in the nanosecond range) is comparable to the timescales of many processes that take place in membranes, thus allowing the use of fluorescence methodologies to obtain dynamical information. Some aspects of this technique which will be encountered in several applications discussed in the present review will be briefly introduced in this section.

Excimers

Some fluorophores, and particularly pyrene, have the property of forming excimers, i.e., transient dimers between an excited and a ground-state probe [38, 59]. This phenomenon is useful to study membrane dynamics, because its probability depends on the likelihood that an excited fluorophore encounters another probe during the lifetime of its excited state, which in the case of pyrene is rather long (in the order of hundreds of nanoseconds). In experiments with membranes, employing lipid analogues labeled with pyrene, this probability is determined by the lateral mobility of the labeled lipids, and by their local concentration. In the case of pyrene, excimers can be spectrally discriminated because they emit with a structureless band centered at around 480 nm, i.e., well separated from the normal emission, which is centered at about 380 nm. Therefore, the ratio of the excimer to monomer emission intensities can be used to sense

variations in membrane fluidity, and possible domain formation, which increases the local concentration of labeled lipids as a result of their co-segregation.

Förster resonance energy transfer

In Förster resonance energy transfer (FRET) an excited fluorophore (donor) transfers its excess energy to another chromophore (acceptor) [60, 61]. The FRET efficiency E is defined as the fraction of excited donors that undergo this process, and can be measured by the decrease in donor's emission intensity or lifetime, or by the increase in acceptor fluorescence. If donor and acceptor are randomly oriented with respect to each other, E depends on the interprobe distance R according to the following equation:

$$E = \frac{1}{1 + \left(\frac{R}{R_0}\right)^6} \quad (1)$$

Here R_0 is a parameter called the Förster radius, which depends on several properties of the probes (particularly their spectral overlap) and is typically a few nanometers. For instance, R_0 is 2.6 nm for the tryptophan–NBD (7-nitro-2-1,3-benzoxadiazol-4-yl) donor–acceptor couple [20]. The hypothesis that donor and acceptor are randomly oriented might not be strictly correct in the case of intramolecular transfer or when the donor and acceptor molecules form a tight, well-defined complex. However, for most of the applications described here this is not the case, Eq. 1 is essentially correct, and the FRET efficiency does not depend on interprobe orientation. Equation 1 implies that the efficiency is practically 1 when $R < R_0/2$ and it is essentially 0 when $R > 2R_0$. For this reason, FRET is a very good tool to measure lipid–lipid or lipid–peptide proximity, because the interprobe distance R can be derived from the measurement of E.

Anisotropy

Fluorescence anisotropy allows the characterization of rotational motions of fluorophores [58, 61]. In these experiments, the sample is excited with linearly polarized light, thus selecting preferentially molecules that are oriented with their transition dipole along the direction of polarization. After excitation, these molecules rotate diffusively and therefore at the time of emission they are more or less randomly oriented, depending on the rate and amplitude of their rotational diffusion, compared to the lifetime of the excited state. The degree of order of the excited molecules at the time of emission can be determined by measuring the polarization of the emitted light. Specifically, anisotropy r is defined as

$$r = \frac{I_{\parallel} - I_{\perp}}{I_{\parallel} + 2I_{\perp}} \quad (2)$$

where $I_{\parallel}$ and $I_{\perp}$ are the intensities of fluorescence with polarization parallel or perpendicular, respectively, to the polarization of the exciting light. This value is maximum when the probe's dynamics is restricted and/or slow (compared to the fluorescence lifetime), and approaches zero when the fluorophore's motions are fast and with a large amplitude.

Labeling

Many of the experiments described in this review require the AMP to be fluorescent, even though studies of the peptide-induced effects on the membrane properties do not suffer from this limitation. Fortunately, several peptides are intrinsically fluorescent, because they contain a tryptophan (Trp) or tyrosine (Tyr) residue. The emission spectrum of Trp is strongly dependent on the environment's polarity (its maximum can range from about 310 to 350 nm), and this property is useful to follow peptide–membrane association [58]. The emission of Tyr, on the other hand, is much weaker, and becomes useful only in peptides lacking Trps. Furthermore, the Tyr spectrum does not shift appreciably when the polarity of the probe's environment changes, being always centered at approximately 305 nm. However, the intensity and lifetime of Tyr emission are sensitive to the fluorophore's surroundings [62].

When the natural peptide does not contain any aromatic residues, analogues can be synthesized in which these amino acids are introduced at specific positions, or alternatively the peptide can be labeled with extrinsic probes. Commonly employed fluorophores in membrane studies are aminonaphthalene or benzoxadiazole derivatives, like dansyl (5-(dimethylamino)naphthalene-1-sulfonyl) or NBD, owing to the extreme sensitivity of their emission spectra to the polarity of the environment [29, 63]. For microscopic studies, extrinsic labeling is a strict necessity, because in this case a strongly fluorescent probe, emitting in the visible range, is needed. Therefore, in these cases, probes like rhodamine and fluorescein are often preferred.

In all cases in which the natural peptide is modified, it is important to check that the labels do not perturb its behavior (e.g., by comparing its membrane-perturbing activity to that of the natural peptide) [20, 64].

By contrast to peptides and proteins, lipids are not intrinsically fluorescent, but several membrane probes such as DPH (1,6-diphenyl-1,3,5-hexatriene), Laurdan (6-dodecanoyl-*N*,*N*-dimethyl-2-naphthylamine) and fluorescent lipid analogues (e.g., labeled with pyrene, NBD, or rhodamine) are available [38, 39].

Membrane models

Although fluorescent approaches are very versatile and in many cases are easily applied to live-cell experiments, in this review we will focus only on studies performed on model membranes [65]. Depending on the specific experiment, different model systems can be used. "small unilamellar vesicles" (SUVs) are liposomes with a size of less than 50 nm, prepared by sonication. Owing to their small size, they have the advantage of scattering light less than other vesicles, but because of their strong curvature the bilayer is strained [66]. Therefore, a better model system is provided by so-called "large unilamellar vesicles" (LUVs), i.e., liposomes with size 50–500 nm, produced by multiple extrusions through membranes with pores of the desired radius [65]. For microscopy experiments, on the other hand, the best model system is provided by "giant unilamellar vesicles" (GUVs), i.e., liposomes with a size in the micron range, that can be imaged by conventional fluorescence microscopy [67]. The best method of preparation of these liposomes is electroformation, which has been shown to produce a high yield of monolamellar, defect-free vesicles [68]. Although this method is best applied in the absence of salts, protocols for GUVs preparation using natural lipids and/or under physiological ionic strength conditions have been described [68].

MD

Molecular dynamics (MD) simulations consist in a numerical integration of the classical equations of motion. In the most common approach, the all atoms (AA) simulation, a molecular system is defined by the position of all its atoms. Given a starting conformation and a set of parameters defining the interaction potential between the different atoms (force field), the forces acting on each of them are calculated. From these, accelerations, velocities, and ultimately the coordinates of the atoms as a function of time can be derived. The final result is a "movie" of the motions of the system, providing an atomic-resolution picture of its structure, dynamics, and function. Obviously, the reliability of the results depends on the approximations introduced, on the parameters of the force field used, and on the time sampled in the simulation. Therefore, an experimental validation is essential.

Coarse graining

A system formed by a bilayer membrane, the surrounding water, and one or more peptide molecules typically comprises several thousand atoms. The computational power presently available usually allows the calculation of the trajectory of such a large system for times of the order of hundreds of nanoseconds. This is often too short to ensure a good sampling of the conformational space, particularly when diffusion through the membrane has to be sampled. Probably, the most important improvement regarding this problem was the introduction of so-called coarse-grained (CG) force fields [69–77]. In the CG-MD simulations, small groups of neighboring atoms, with similar properties or belonging to the same chemical group, are treated as a single particle, thus reducing the number of forces to be calculated in the simulation, and making longer trajectory timescales accessible. The CG approximation loses some details of the simulated system, but it allows a better sampling of the conformational space. Because the latter can be the main limitation in simulations of membrane systems, CG studies often correlate with experimental data better than AA simulations [78]. However, the critical point in this approach is the definition of the force field parameters. In recent years, several approaches were proposed to obtain CG descriptors for biological systems (and for lipids in particular), based on fitting of data obtained from AA simulations [72–74] or from thermodynamic experiments [71, 76]. Nowadays, the available CG force fields produce simulations in good agreement with the available experimental evidence, and provide a speedup of 2–3 orders of magnitude in comparison with AA simulations, not only as a result of the obvious reduction in the number of particles to be considered, but also because the removal of the fastest degrees of freedom allows the use of much longer time-steps in the numerical integration of the equation of motion (typically 40 fs, instead of the usual 2–4 fs used in AA simulations) [76].

Potential of mean force

In addition to coarse-graining approximations, many other methods have been proposed to overcome the problems related to a poor sampling of complex systems, usually based on the identification of a global coordinate, as in the case of the potential of mean force (PMF) evaluation. The PMF, introduced by Kirkwood [79], is defined as:

$$W(\xi) = -k_B T \ln\langle\rho(\xi)\rangle \quad (3)$$

where ξ is the global coordinate and $\langle\rho(\xi)\rangle$ is the average of the distribution function at ξ fixed but averaged over all the other degrees of freedom. $W(\xi)$ defines the free energy profile with respect to the coordinate ξ. In principle, standard MD simulations could be used to evaluate this function, but processes involving high free energy barriers require times which are often too long to be efficiently sampled. In this case, the most used method to generate a reliable PMF is the umbrella sampling [80], in which the system is forced to sample regions of the conformational space that would not otherwise be accessible in the

simulation time, with conventional sampling. For example, the reaction coordinate could be the distance between the peptide and the center of the bilayer. To force the sampling of conformational states along this coordinate, which would otherwise be poorly populated, different biased trajectories, with the peptide constrained at defined distances from the membrane center, are carried out. After acquiring these biased ensembles an opportune treatment is needed to obtain unbiased parameters [81–83]. The final results of these simulations are the ensemble of conformations spanning the whole insertion pathway and the free energy profile as a function of distance from the center of the bilayer. From this, the most stable position of the peptide inside the membrane can be easily deduced. The PMF analysis requires a complete sampling and equilibration of the system at each of the depths of insertion studied. This is a demanding requirement, but it can be tested in several ways [83]. Furthermore, the PMF profile can be calculated both reducing the peptide–membrane distance and increasing this parameter. The presence of a significant hysteresis is indicative of poor sampling [84].

Membrane models

Regardless of the selected approach, usually just a small slab of bilayer is included in simulations of membrane systems, ranging from a few hundred lipids for AA simulations to a few thousand for CG simulations. Recently, CG simulations of whole vesicles became feasible, and allowed studies on the effect of membrane curvature on the activity of the maculatin peptide [85]. From a computational point of view, an attractive alternative to bilayers is represented by micelles, which are computationally less demanding and are also often used in NMR experiments [86, 87]. However, it is debatable whether they represent a good model of bilayer membranes [50].

Structural parameters

A quantitative analysis of MD trajectories allows the calculation of several structural and thermodynamic parameters. For instance, in simulations of peptide–membrane systems, it is possible to calculate the membrane thickness and the degree of order of the lipid chains, to observe the effects of peptide binding on these quantities. Bilayer thickness can be evaluated as the distance between the average z-coordinates of the phospholipid phosphate groups.

The lipid order parameter is defined as:

$$S(n) = 1/2\langle 3\cos^2\theta_n - 1\rangle \quad (4)$$

where θ_n is the angle between the nth segmental vector linking carbon C_{n-1} and C_{n+1} in the acyl chain and the normal to the bilayer, and the brackets denote an ensemble average. The lipid order parameter is particularly useful for comparison with experimental data, because it can be measured by NMR techniques, and estimated by time-resolved fluorescence anisotropy experiments. From a computational point of view it can be calculated directly from AA-MD. Similarly, an order parameter for lipid chains can also be calculated for CG simulations; in this case θ represents the angle between consecutive beads and, obviously, only qualitative comparisons with experimental data are possible.

Water–membrane partition

Fluorescence

The first information that can be obtained through fluorescence spectroscopy experiments is the affinity of the peptide for membranes. These data are extremely relevant, because association to membranes is a major determinant of the overall peptide activity [7, 64]. By comparing experiments with model membranes of different composition, useful information on peptide selectivity can also be obtained, because the lipid mixture is different in bacterial and eukaryotic cell membranes. In addition, in many of the experiments described in the following sections (e.g., FRET measurements of peptide aggregation, or quenching experiments) it is essential to know the fraction of membrane-bound peptide, and the conditions that ensure complete association to the bilayer.

There are many different fluorescence observables that can be exploited to follow the association process [40, 44, 88]: intensity, wavelength, anisotropy, lifetimes, FRET efficiency. Each of them reports on a different physical phenomenon, so that they are complementary, and the best experimental approach can be selected depending on the specific system under investigation. Emission intensity usually is significantly enhanced by membrane binding, as a result of the more viscous nature of the bilayer (as compared to the water solution), thus reducing the rate of nonradiative decays. Peptide association to a bilayer is typically followed by a significant blue shift of its fluorescence spectrum, as a result of the lower polarity of the membrane environment. In addition, attachment to the relatively large lipid vesicles severely hinders the diffusive motions of the peptide, thus causing a significant increase in its fluorescence anisotropy. If the membrane is labeled, its fluorophore can act as an acceptor for the peptide fluorescence, and in this case the FRET efficiency will increase after binding. In addition, even if the peptide is not fluorescent, its membrane association can be detected indirectly by following its effects on the membrane properties.

It is important to stress that a quantitative determination of the partition constant can be obtained only from those variables that are additive [88, 89]. This means that, if we have two possible states for our fluorescing molecule, e.g., peptide in water (W) and peptide in the membrane (M), the measured value of the observed variable S will be given by

$$S = S_M f_M + S_W(1 - f_M) \quad (5)$$

where f_i is the molar fraction of molecules in state i, and S_i is the signal measured (under the same experimental conditions) with all molecules in state i. This additivity property is not general. For instance, the fluorescence intensity at a fixed wavelength and the average lifetime (amplitude weighted [44]) are additive, and thus allow a quantitative determination of the partition constant, whereas the spectral shift is not, and therefore it only provides a qualitative assessment of peptide–membrane association. Anisotropy follows Eq. 5 only in the case in which the quantum yield in the two states is the same [89].

If the additivity condition is met and if the peptide populates only two states (monomer in water and in the membrane) the fraction of membrane-bound peptide can be calculated by rearranging Eq. 5:

$$f_M = (S - S_W)/(S_M - S_W) \quad (6)$$

Usually, the peptide is titrated with increasing concentrations of vesicles, and the fraction of membrane-bound peptide is determined for each experimental point. The best formalism to treat these data is as a partition between two immiscible phases (water and membrane) [88]. In this case, it can be shown that the fraction of membrane-bound peptides depends hyperbolically on the lipid concentration:

$$f_M = \frac{K[L]}{1 + K[L]} \quad (7)$$

However, Eq. 7 is based on the hypothesis of an ideal behavior. Significant deviations are expected as soon as the peptide concentration in the membrane increases. Obviously this formalism is also inadequate in all those cases in which electrostatic interactions are significant, as is often the case with cationic AMPs and anionic bacterial membranes. In this case, the Gouy–Chapman model is more appropriate [90]. Other instances in which Eq. 7 fails are cases in which the two-states hypothesis breaks down, as in those cases in which the peptides aggregate. Equation 7 has a striking property that can be exploited to test its adequateness in the case under study: it does not depend on peptide concentration. Therefore, two curves measured at different peptide concentrations should overlap. Otherwise, more complex models should be employed [64, 91]. For instance, in the case of the peptaibol trichogin GA IV, the observation that binding curves measured at different peptide concentrations were not superimposable, and exhibited a sigmoidal behavior, was the first indication of the presence of peptide aggregates both in water and in the membrane; these aggregates were successively demonstrated with other approaches [64].

MD

The water–membrane partition process can also be studied by means of MD simulations [92], which can produce an estimate of the partition free energy difference. Even though this quantity is easily and reliably measured experimentally, as described above, a comparison between the theoretical and experimental data is extremely useful to validate and refine the simulation parameters. For instance, the MARTINI force field, which is one of the main CG force fields for the simulation of membrane systems, was parameterized by optimizing its ability to reproduce free energies of partition between polar and apolar phases [93]. An efficient simulative estimation of the partition constant is also useful in the in silico rational design of peptide analogues with improved characteristics. Furthermore, computational partition studies provide a structural picture of the membrane insertion process. The best approach to characterize peptide–membrane association is to calculate the PMF, usually by umbrella sampling methods. As stated in a previous section, this technique leads to the calculation of the free energy profile along a global coordinate, which in this case is the distance of the peptide from the membrane center. It also gives the opportunity to separate, for each sampled peptide position, the different energetic contributions (hydrophobic or electrostatic) of the peptide–lipid interactions, as done in the case of the peptide voltage sensor toxin 1(VSTx1) [83]. Therefore, in addition to the partition free energy, this type of analysis also defines the most stable position of the peptide inside the membrane, as further discussed in the next section.

Peptide position in the bilayer

Fluorescence

Another important aspect in the determination of the mechanism of membrane destabilization by AMPs is their position inside the membrane. Fluorescence can provide important information regarding this point. Obviously, fluorescence reports on the position of the fluorophore, rather than that of the whole peptide. However, by studying several analogues in which the fluorescing residue is placed at different positions along the sequence, the depth of

insertion and the orientation of the peptide can be determined [20].

The first, very simple information one can get about peptide insertion can be obtained by looking at the spectral shift of the fluorescence caused by membrane association. This property can be exploited to discriminate between fluorophores that, after membrane association of the peptide, remain in water, are at the surface of the membrane, or are inserted in the hydrophobic core of the bilayer, as exemplified by our studies on PMAP-23 and alamethicin [20, 94].

Another possibility to obtain more detailed information is to measure the effect on the emission intensity of water-soluble "quenchers," i.e., molecules which can cause the nonradiative decay of an excited fluorophore by collisional encounter. The most prominent examples are acrylamide and iodide. Because these molecules act by short-range, contact mechanisms, their efficiency depends on the accessibility of the fluorophore, and therefore it can be used to obtain information on its depth in the membrane. Usually, fluorescence intensity is measured as a function of the aqueous quencher concentration [Q], and data are reported in a so-called Stern–Volmer plot [58] of $(F_0/F) - 1$ versus [Q], where F is the fluorescence intensity measured in the presence of a given quencher concentration, and F_0 is the emission intensity in the absence of any quencher. In the simplest case of a homogeneous sample in which the fluorophore populates a single depth, a linear relationship is expected [95]:

$$\frac{F_0}{F} = 1 + K_{SV}[Q] \tag{8}$$

Here K_{SV} is called the Stern–Volmer constant, and is given by $k_q\tau_0$ where k_q is the bimolecular quenching constant, which depends (in addition to other parameters) on the solvent accessibility of the quencher, and τ_0 is the fluorophore's excited state lifetime in the absence of the water-soluble quencher [58]. For comparison, the same plot should be measured for a completely water-exposed fluorophore, such as Trp in water.

More detailed data on the fluorophore's position in the bilayer can be obtained by using quenchers that are inserted in the membrane and located at a specific depth (Fig. 1a). These can be phospholipids or fatty acids labeled with bromine atoms or doxyl groups [37]. All these quenchers act at short range (a few Ångströms) [96]. Therefore, the quencher whose depth in the bilayer is closer to that of the fluorophore will cause the maximal quenching (depth-dependent quenching, or DDQ). Experimentally, the peptide is incubated with liposomes containing lipids labeled at different positions (and, for reference, to unlabeled vesicles) and the quenching is compared. In the simplest possible approach, the probe position is assumed to correspond to that of the label causing maximal quenching. Other more sophisticated methods ("parallax" or "distribution" analysis) use some form of fitting of the so-called quenching profile, i.e., a plot of the quenching as a function of the quencher depth in the bilayer [37].

Water-soluble and membrane-attached quenchers can be combined in order to determine a fluorophore's depth in the bilayer. For instance, Caputo and London [97] showed that the ratio of acrylamide quenching to that of 10-doxylnonadecane is nearly linearly dependent on the depth of the fluorophore in a membrane. Finally, it is worth mentioning that the possibility of performing the same measurements in GUVs has been demonstrated [98].

These types of quenching measurements are extremely important to determine the peptide's mechanism of action. For instance, these experiments demonstrated that the peptaibol trichogin GA IV binds at the membrane surface at low peptide/lipid ratios, and inserts in the bilayer as the membrane-bound peptide concentration increases [99]. By contrast, similar measurements demonstrated that the cationic AMP PMAP-23 always remains on the membrane surface [20].

Another important aspect of peptides' interaction with membranes is whether they are able to cross the bilayer (translocate) and distribute in both leaflets of the membrane (or to access the inner aqueous volume of vesicles) [11]. Fluorescence methods can clarify this aspect as well. Although several approaches utilizing fluorescence have been used to assess peptide translocation in cells [41], here we will discuss only approaches that can be applied to model membranes, without trying to be exhaustive (for a comprehensive review, see [41]).

The simplest method is obviously direct visualization of giant vesicles by confocal microscopy [100]. However, this approach requires peptide labeling with an extrinsic fluorophore, which in principle can significantly perturb the translocation behavior of the peptide [101]. Furthermore, GUVs have been demonstrated to give rise to translocation artifacts in some cases [102].

The best way to determine the amount of peptide associated to both membrane layers exploits FRET [99] (Fig. 1b). If a FRET acceptor for peptide fluorescence is inserted in the membrane, and the Förster radius is less than the bilayer thickness (about 4 nm), then the FRET efficiency will be significantly different if the peptide and acceptor are in the same or in different leaflets. Matsuzaki et al. [103] and Wimley and White [104] first pioneered this approach to assess translocation by comparing the FRET efficiency when peptides were associated to vesicles labeled in both layers, or in the outer layer only. We improved this approach by introducing a third type of vesicles, i.e., liposomes labeled in the inner leaflet only [99]. A scheme of the expected differences in FRET

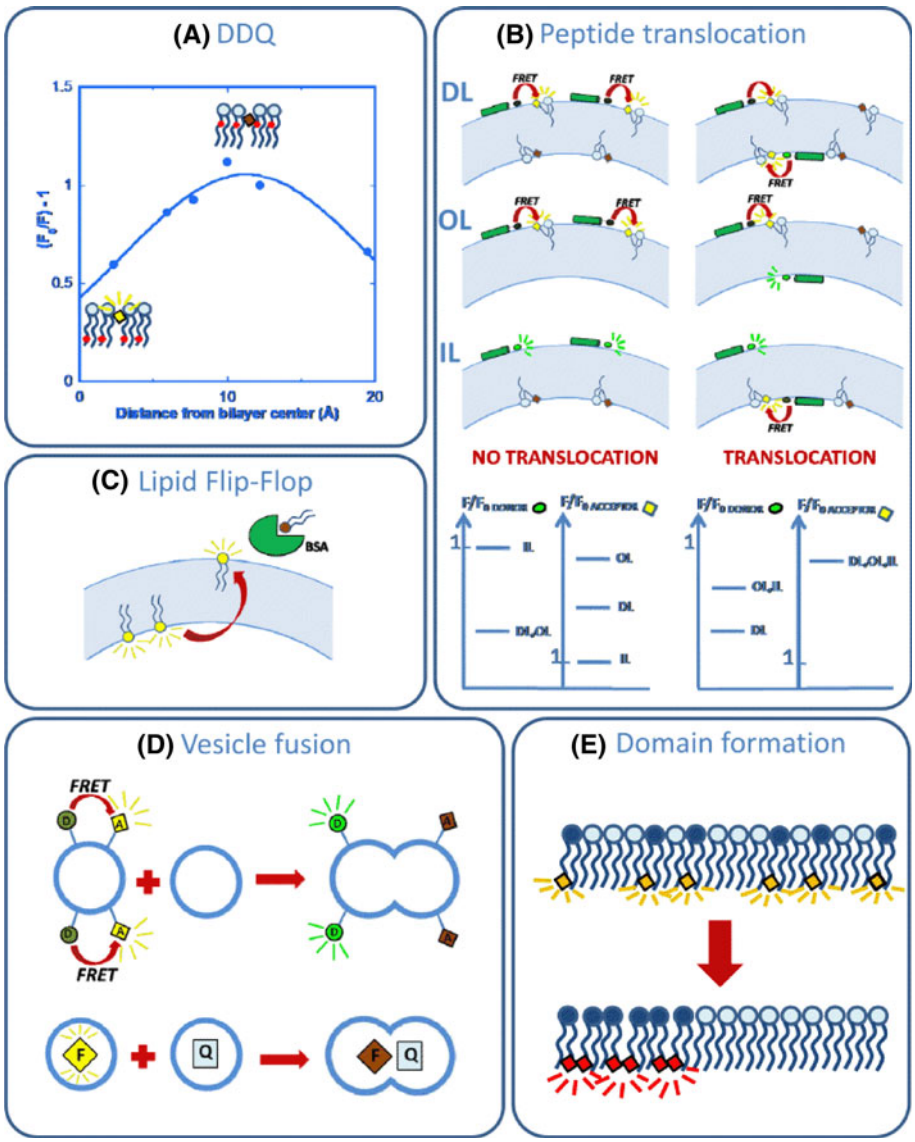

Fig. 1 Schematic depiction of some of the fluorescence assays described in this review. **a** DDQ. The depth-dependent quenching assay allows the determination of the depth of insertion of a fluorescing peptide (represented as a *square*) inside the bilayer. DDQ employs lipids labeled with a quenching group (depicted as a *red dot*) at a specific position on the acyl chain. Maximal quenching is observed when the depth of the quencher and of the fluorophore in the membrane coincide. Typical quenching data are shown in the plot, as a function of the distance of the quenching group from the bilayer center. **b** Translocation. In order to verify if a peptide (*green cylinder*) is able to translocate across the bilayer, three vesicle preparations are employed: "double labeled" (*DL*), with fluorescent lipids on both layers; "out-labeled" (*OL*), or "in-labeled" (*IL*), with fluorescent lipids on the outer or inner layer only, respectively. These lipids can act as FRET acceptors to the peptide fluorescence. The figure describes the decrease in peptide fluorescence (F), when interacting with these three types of liposomes, with respect to a sample containing unlabeled vesicles (F_0), where energy transfer is absent. Similarly, the increase in lipid fluorescence caused by peptide binding is represented. The scheme in the *lower panel* reports the intensity variations expected for the different vesicle preparations in the absence and in the presence of peptide translocation. **c** Lipid flip-flop. In this assay, BSA is added in the water solution outside vesicles. This protein is able to extract fluorescent lipids from the membrane, quenching their emission. Labeled lipids associated to the inner leaflet become accessible to BSA only after they flip-flop to the outer layer. **d** Vesicle fusion. To measure lipid exchange, vesicles labeled with FRET donors and acceptors are mixed with unlabeled liposomes. Fusion causes an increase in the average donor–acceptor distance, and a decrease in FRET efficiency. To measure mixing of the vesicles' aqueous contents, liposomes entrapping a fluorophore are mixed with vesicles containing a quencher. Fusion causes the encounter of these two molecules and a decrease in fluorescence. **e** Domain formation. Pyrene-labeled lipids are used in this assay. When they co-localize as a consequence of domain formation, excimers are formed, causing a variation in the wavelength of the emitted fluorescence

efficiency in the presence or in the absence of translocation is shown in Fig. 1b. This determination of peptide translocation is quite robust, because it compares four different vesicle populations (internally, externally, and symmetrically labeled, plus unlabeled liposomes), and detects both the decrease in donor (peptide) fluorescence and the increase in acceptor (labeled lipid) emission due to FRET. The asymmetry of vesicle labeling is an essential part of this assay. Because it would be rapidly destroyed by lipid flip-flop, which is often favored by membrane-active peptides [105], this phenomenon should be characterized in detail before the assay can be employed (see below for flip-flop studies).

By using this method, we recently demonstrated that at concentrations too low to induce pore formation, some AMPs (like trichogin GA IV) are able to translocate across the membrane, whereas others are not [28]. This point is relevant for the peptide's mechanism of action because only peptides that do not translocate can build up a difference in surface tension between the two leaflets of the bilayer, as required by the carpet mechanism.

A novel approach to detect translocation has been proposed by Keller and co-workers [106], and it does not suffer from the limitations related to peptide-induced lipid flip-flop. This assay exploits the reversibility of peptide–membrane binding: peptide–vesicle dissociation is induced by diluting the sample, and it is followed by recording variations in fluorescence spectra. Dissociation in different liposome preparations are compared: vesicles co-prepared with the peptide (that therefore is necessarily distributed in both layers), and vesicles to which the peptide was added from the outer phase. If the peptide can translocate, in both cases dilution will ideally lead to the dissociation of the whole peptide. If, on the other hand, the peptide is unable to cross the membrane, part of it will remain entrapped inside the co-prepared vesicles.

MD

The determination of peptide position inside a bilayer is one of the main goals of MD simulations of peptide–membrane systems. The classical way to determine the most stable conformation of an AMP inside the membrane is to start with the peptide in water, in the presence of preformed bilayer. Extensive simulation of this system can lead to the spontaneous association of the peptide to the membrane and to its eventual insertion in the bilayer [107]. In principle, these simulations should be continued, in an unbiased way, until the peptide reaches a stable conformation inside the membrane, but usually this process is too slow to be exhaustively explored. Therefore it is impossible to exclude that the system is metastably trapped in a local free energy minimum.

In order to reduce problems related to poor sampling of the conformational space, constraints can be added to the simulation to pull the peptide from the water solution to the center of bilayer. These biased simulations can provide the PMF profile as a function of peptide distance from the membrane center. From this, the most stable position of the peptide inside the membrane is easily deduced. PMF calculations have been successfully applied to determine the position and conformation of peptides in lipid bilayers [84, 108, 109], providing an atomic-resolution picture of the membrane-inserted state that is unattainable experimentally. In addition, PMF analyses give a picture of the whole insertion pathway, including the conformations corresponding to the potential energy barriers to the insertion, or to local minima in the insertion pathway. These can be used to design new peptides with different characteristics [110].

A completely different approach to find the most stable conformation and position of a peptide in a membrane was recently proposed. Studies published in the last decade had shown that a random mixture of water and lipids spontaneously self-assembles into a bilayer, usually in less than 100 ns of simulated trajectory [111–114]. The assembly process proceeds through consecutive steps: in a few nanoseconds, clusters of lipids are formed; then, in tens of nanoseconds they assembly in a disordered bilayer, in which usually one or more water-filled pores are still present. In this time the lipids can flip-flop and eventually homogenize their distribution between the two leaflets. After this step, the pores close and an ordered bilayer is formed, but several nanoseconds of simulation can be needed before this takes place. A critical parameter in this context is the number of water molecules considered during the simulations; a higher number of water molecules can reduce the time of closure for the system. Obviously, a compromise with the need to reduce the computational time has to be found, and usually a water/lipid ratio in the range 40–60 has been used in AA simulations. Furthermore, it has been shown that bilayer defects can be eliminated with an annealing treatment in which the temperature is cyclically increased and decreased [20, 28]. Recently, this same self-assembling approach was applied to a random mixture of water and lipids, also including one or more peptides [17, 115, 116]. In this way the simulation is not biased by the starting configuration of the system. In addition, although the penetration of a peptide in a preformed bilayer is slowed down by the relatively viscous and ordered membrane environment, the system is much more fluid during the self-assembly process, when a regular bilayer is not formed yet. This ensures that the peptide can experiment different environments in a relatively short time, and, as a consequence, it is more likely to find its minimal free energy configuration. This approach has been

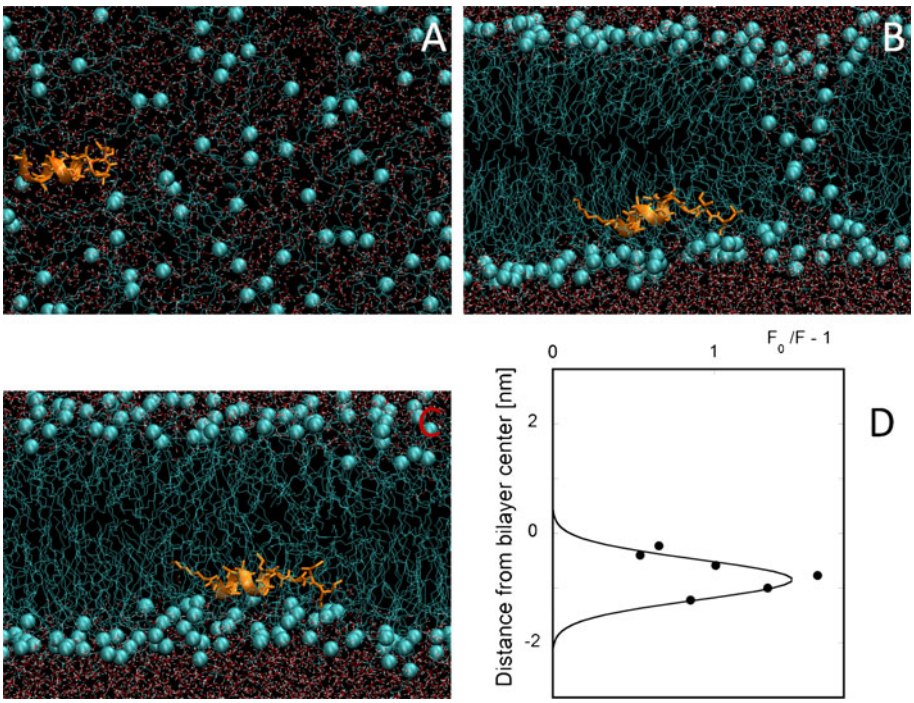

Fig. 2 Different steps along an AA-MD simulation of membrane self-assembly in the presence of the peptide trichogin GA IV [28]. **a** Initial random distribution of lipids, water, and peptide. **b** Spontaneous formation of a bilayer, still containing a water-filled defect. **c** Final defect-free bilayer. **d** Experimental DDQ profile, reported for comparison of the experimentally determined peptide position with that resulting from the simulation. Lipids are represented in *cyan*, with their phosphate atom reported as a *sphere*. The peptide is in *orange*, and the water molecules have their oxygen atoms colored in *red*, and their hydrogens in *white*

applied to several peptides, both at the CG level [85, 93, 115, 117–119], and with AA resolution [17, 20, 28, 116]. In these studies, both transmembrane and interfacial configurations have been observed, with different peptides [28, 116], and, in some cases, the reliability of these predictions was confirmed by comparison with DDQ experiments (Fig. 2) [20, 28].

The two approaches (preformed bilayer and self-assembly) have a key difference with respect to the peptide effects on lipid distribution. Many AMPs exert their activity by associating to the surface of the external layer of the cell membrane, thus creating a difference in the surface tension of the two leaflets of the bilayer. This tension is then released by creating a membrane defect, so that some lipids can translocate from the external to the internal layer. This is the main driving force of the "carpet" model of peptide-induced leakage. This property of some peptides is easily evidenced by self-assembly simulations, because, in the presence of membrane defects, lipids can easily translocate from one layer to the other. As a consequence, when the membrane defect heals, a different number of phospholipids is present in the two leaflets, with less lipids in the layer where the peptide is located. This difference can be used to estimate the effect of the peptide on the surface tension of the membrane [28]. It is interesting to note that peptides that adopt a transmembrane orientation, or that do not act according to the carpet mechanism, do not cause this asymmetric distribution of lipids. For instance, the cationic, surface-bound peptide PMAP-23 induced a difference in the number of lipids between the two leaflets of about 15%, whereas this difference was negligible in the case of trichogin GA IV [28]. The redistribution of lipids between the two membrane layers is not easily attainable in a conventional simulation starting with a preformed bilayer, because lipid flip-flop in a defect-free membrane is a rare event that is not usually sampled in the simulation times [120]. This represents a barrier to peptide insertion inside the membrane, so that peptides usually remain for a long time in an excessively superficial position in simulations of preformed bilayers. On the other hand, the accumulated stress in this type of simulation is usually witnessed by a higher flexibility of lipids in the leaflet where the peptide is located, for example, in terms of planarity of the polar heads in simulations of melittin [18]. This stress can favor the observation of peptide-induced membrane defects (see below), and it could explain the anomalous amount of unfolded peptide structure detected, for example, in similar simulations carried out on the peptide magainin [17]. By contrast, self-assembly simulations lack this driving force for membrane permeabilization, and therefore are less useful for observing the mechanism of pore formation. In any case, it is important to note that, when a single peptide is simulated with 100–200 lipids, the peptide to lipid ratio might be lower than that needed for membrane activity. Furthermore, the absence of other peptide molecules impairs the occurrence of peptide–peptide interactions, often needed to permeabilize the membrane. Therefore, simulations containing a single AMP are often representative of an inactive peptide state, irrespective of the

specific approach employed. However, they can be compared to experimental results obtained under similar conditions, and provide an atomic-level picture of the peptide–membrane system under investigation.

Peptide aggregation

Fluorescence

Formation of peptide aggregates has important effects on the membrane-perturbing activity of the peptides. Aggregation in water screens the hydrophobic portions of the peptide sequence and competes with association to the membrane [64, 121]. Aggregation in the membrane may be part of the pore formation process, as in the case of peptides acting according to the barrel-stave model [28, 122]. Fluorescence spectroscopy is an important tool to qualitatively and quantitatively characterize the aggregation processes.

Usually, formation of aggregates will change the environment around the fluorophore, and thus become detectable by changes in intensity, fluorescence lifetime, or spectral position with peptide concentration [64, 121, 123]. Quantitative analysis of fluorescence lifetimes is complicated for intrinsic fluorescence by the nonexponential decay of the Trp fluorophore, even under monomeric conditions. However, in those cases in which the monomeric peptide exhibits a monoexponential decay (as in peptides labeled with fluorene), the pre-exponential factors of the different lifetimes observed in the presence of aggregation provide the relative populations of the different species. For instance, for the trichogin GA IV analogues F10 and F0, with a global analysis of the fluorescence decays, we were able to measure the population of the four different species formed by these peptides (monomers and aggregates, both in water and in the membrane) [64, 121, 123] (Fig. 3). Direct interaction of the fluorophores in the aggregates is also possible, with the formation of dimers or excimers, which have different spectral properties as compared with the monomeric label, particularly if the fluorophore is pyrene [124]. However, the most sensitive method to unambiguously detect peptide aggregation is FRET [42, 99]. In this case, two peptide samples are labeled with two different fluorophores (that can act as a FRET donor–acceptor couple), and then mixed in different proportions; aggregation results in measurable FRET. In studies of aggregation in membranes, the measured FRET efficiency should always be compared with the nonzero values expected for a random distribution of donors and acceptors in the bilayer [99, 125], as a result of random encounters between the two probes. However, it should always be considered that an observed FRET efficiency higher than that expected for a random distribution could be due to co-localization in membrane domains rather than to real aggregation [126].

MD

Although fluorescence experiments can demonstrate the formation of aggregates, they usually cannot determine their size or architecture. Therefore, computer simulations of the aggregation process are particularly useful. Simulations of peptide self-association in water are very common, but usually refer to fragments of amyloid proteins [127], or to artificial peptides designed to self-assemble in nanostructures [128], and only in a few cases they concern aggregation of AMPs [77]. Simulations of AMPs are mainly focused on the aggregation process inside lipid bilayers, and we will limit our discussion to these studies. This problem has been intensely investigated in the last 10 years [107, 129–131], because it is an essential step in the pore formation process, both in the barrel-stave and in the toroidal model. Even though this topic is technically challenging, because of the timescale and system size involved in the simulation of the formation of functional aggregates, the picture that comes out from the many published papers is of substantial agreement between the simulation and the available experimental results.

Simulating the global process leading to the formation of aggregates in the membrane, starting from the peptides

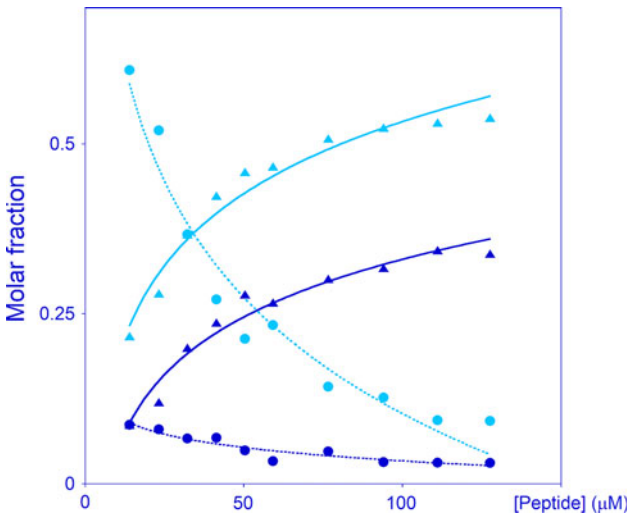

Fig. 3 Molar fraction of the different species populated by the fluorescent trichogin GA IV analogue F10 in the presence of liposomes (2 mM lipid), as a function of total peptide concentration, as determined from a global analysis of the fluorescence time-decays of the fluorene fluorophore. The four species are monomeric peptide in water (*dark blue circles*, lifetime 5.6 ns), monomeric peptide in the membrane (*light blue circles*, lifetime 7.0 ns), aggregated peptide in water (*dark blue triangles*, lifetime 0.87 ns), and aggregated peptide in the membrane (*light blue triangles*, lifetime 2.2 ns) [64]

in water, is very demanding. Two strategies have been adopted to reduce the computational complexity: (a) preassembled aggregates are simulated to study their stability and structural and functional features; (b) monomeric peptides are embedded in the membrane and their spontaneous self-assembling process is simulated.

Some of the first attempts to simulate active pores in bilayers consisted of simulations of preassembled alamethicin aggregates [122]. A barrel-stave structure had been convincingly demonstrated experimentally for this peptide, and this allowed the manual assembly of putative pores. The goal of these simulations was therefore to determine the most stable aggregate size, and the functional properties of the pores, such as conductance or ion selectivity. For instance, Tieleman et al. [122] carried out AA simulations of several tens of nanoseconds on different putative alamethicin channel structures, to individuate the most stable configuration. In this way the authors proposed a structure in terms of a regular pore comprising six peptides, in agreement with the conductance levels measured in experiments with planar bilayers. Even though this approach has now been applied to other peptides [132, 133] it always needs to be based on one or more competing hypotheses of the pore structure, and therefore it is better suited to molecules supposed to form ordered transmembrane barrel-stave pores. Insertion of peptides into a preequilibrated bilayer can take place only after a proper removal of lipids to make space for the peptides, either manually or driving them out with a weak repulsive potential. A different approach has also been proposed in which the starting structure is obtained by placing the peptides in a bilayer with increased lipid–lipid spacing. After inserting the peptides among the lipids, the bilayer is compressed to reach the physiological density. A web resource is available with many tools that can be used to help in the preparation steps [134]. For an exhaustive review of these methods, see [135].

Simulations of the self-assembling of membrane-inserted peptides ensure an unbiased structure for the aggregates, but require long simulation times, and are therefore usually performed with the CG method [136]. Recently, a multiscale approach has been proposed, in which different steps have been simulated at CG or AA resolution to ensure the optimal compromise between the need to perform an efficient sampling of the conformational space and the need to simulate the key steps at atomic resolution [136–138]. Generally, CG simulations are used to simulate the diffusion of several peptides in the membrane, leading to the formation of aggregates. Successively, the simulation is continued at AA resolution. This approach is promising to overcome the limitations of the CG approximation, and it provides an opportunity to directly compare AA and CG results. For instance, in the simulation of alamethicin–membrane interaction by Thøgersen et al. [137], water molecules were able to diffuse trough the channel at the AA level, but not in the CG simulation. In addition, partial unfolding of a few peptides was observed in the AA-MD, whereas the CG approximation favors structural stability. NMR and X-ray data indicate that this multiscale approach can lead to correct structures. However, the conversion of the simulations from CG to AA is a delicate step [139].

The increasing availability of CPU power, and the development of highly efficient computational methods in the MD field allowed, in a few cases, researchers to follow the full process of membrane permeabilization, even at the AA level, and starting with the peptides in water. Sengupta et al. [18] simulated the permeabilization of a bilayer by melittin in several simulations (for a total trajectory length of more than 2.5 μs) carried out under different conditions (number of lipids, peptides, ions, etc.). Even though pore formation is a stochastic process and can take place after different simulation times [17], it is influenced by the simulation conditions, like the number of counterions. This method allows an unbiased determination of the pore structure, and is also easily applied to peptides that do not insert in a transmembrane orientation, unlike the other approaches described above.

In general, the picture of AMPs' pores resulting from simulation studies is more disordered than expected, for peptides acting according to the toroidal pore model [18, 140], and even for the barrel-stave channels of alamethicin [137], regardless of the computational approach used. The secondary structure of the peptides involved in pore formation is also a debated issue in the literature. An interesting comparison, in this context, can be done by taking data from two simulations carried out under similar conditions but at different resolution. Marrink and co-workers [17, 93] reported simulations of pore formation by the peptide magainin-H2, using both AA and CG force fields. Although the pore structure was similar in the two cases, the degree of α-helical secondary structure in the peptide was different in the two simulations, with the AA approach underestimating the peptide helicity.

Peptide-induced membrane perturbation

Fluorescence

Permeabilization

One of the most important aspects in the characterization of AMPs is their membrane-perturbing activity. Fluorescence methodologies can reveal the pore formation kinetics, the size of the pores, and the type of membrane leakage mechanism.

The most used method to measure peptide-induced leakage exploits water-soluble fluorophores that at high concentrations exhibit a self-quenching effect, such as carboxyfluorescein, which forms nonfluorescent dimers at concentrations above about 5 mM [20], or calcein. In a typical experiment, the probe is entrapped inside liposomes at a self-quenching concentration, and the free dye is removed by gel filtration. At this point, any leakage of the dye from the vesicles causes its dilution in the outer volume, removal of the self-quenching effect, and a large increase in the fluorescence signal. The advantage of this approach is that it allows one to follow the kinetics of the leakage process. A detailed analysis of these curves can provide important information on the mechanism of the pore formation process. We recently proposed a mechanistic model that was able to reproduce the main features of the observed experimental kinetics, and to provide the average number of open pores per vesicle [141].

An alternative to the carboxyfluorescein method is to co-encapsulate a fluorophore and a quencher, such as disodium 8-amino-1,3,6-naphthalenetrisulfonate (ANTS) and *p*-xylene-bis(*N*-pyridinium bromide) (DPX), inside the vesicles [142]. Alternatively, a luminescent ion with a chelator, such as the Tb^{3+}/DPA (dipicolinic acid) pair [143], can be used. Dilution in the volume outside vesicles, because of peptide-induced leakage, removes the interaction between fluorophore and quencher (or ion and chelator) and causes a change in the fluorescence signal. However, this approach adds an additional complication, because the leakage kinetics of the two entrapped molecules can be different [142].

In order to test the size of the pores, it is possible to entrap fluorescent molecules of different sizes inside the vesicles [144]. Typically, dextrans of various molecular weights are used for this purpose. Fluorescein-labeled dextrans can undergo self-quenching at appropriate concentrations [145], and therefore can be used in the same way as carboxyfluorescein. Pore sizing with this approach requires consecutive experiments in each of which a specific molecular weight dextran is tested. Alternatively, Ladokhin et al. [144] described a method to co-encapsulate different dextrans in the same vesicle, and to assay their leakage in a single experiment, using gel-filtration chromatography to separate the released dextrans.

All the molecules described so far are relatively large (even carboxyfluorescein has a molecular weight of 376 Da), and there have been cases in which a peptide causes pores so small that they are able to induce the leakage of ions, thus leading to bacterial death, but not of these larger fluorophores [146]. In these cases, ion leakage can be tested by entrapping inside the vesicles a fluorophore that binds specifically a given ion (e.g., SBFI, sodium-binding benzofuran isophthalate for sodium, and KBFI, potassium-binding benzofuran isophthalate for potassium), and changes its spectral properties after association [147]. In these experiments, that specific ion is not included in the vesicle preparation buffer, but is part of the buffer in which they are diluted. When the peptide causes ion permeability, the ion can reach the fluorophore, and leakage can be detected by the change in the probe's fluorescence. Of course this approach is specific for the leakage of ions only in those cases in which it has been shown that the fluorophore is not able to leak through the peptide-induced pores.

In addition to experiments exploiting LUVs, leakage can also be easily followed in GUVs, in this case by direct microscopic observation [148]. With GUVs it is very easy to detect the differential leakage of markers of varying molecular weights [141, 149], and recently the leakage kinetics was also studied in detail at the single vesicle level using these liposomes [150].

An important point about the leakage process is whether it is "all or none" or "graded." In the first case, at any given time, some vesicles are completely full, while others have released completely all their contents, or have been destroyed. By contrast, in the second case, partially empty vesicles are present. This distinction reflects the underlying molecular mechanism of pore formation. The two mechanisms are discriminated immediately in a GUV experiment, just by direct observation [20, 141, 151], but in an ensemble experiment like those performed with LUVs it is more difficult to differentiate them. A common approach, used in combination with self-quenching dyes, is to stop the leakage process after some incubation. This can be accomplished by adding to the sample a protease that digests the peptide, or, provided that the peptide-membrane binding is reversible, an excess of lipid vesicles (thus reducing the membrane-bound peptide concentration to a value below the activity threshold). Successively, the released dye is separated from the vesicles by gel-filtration chromatography. At this point, the degree of self-quenching of the dye still contained inside liposomes is determined by measuring the fluorescence intensity before and after the vesicles are broken with a detergent. If the quenching was still the same as the original population then the mechanism is all or none, otherwise it is graded [20].

Vesicle aggregation and fusion

In some cases AMPs also induce aggregation and/or fusion of vesicles [146, 152, 153]. These phenomena can be tracked by FRET measurements (Fig. 1d). Aggregation and fusion can be detected by using two vesicle populations, one labeled with a FRET donor (e.g., NBD-labeled lipids), the other with a FRET acceptor (e.g., rhodamine-labeled lipids). When the two liposome types associate, FRET

occurs [154]. Alternatively, vesicles labeled with donor and acceptor are mixed with unlabeled vesicles; in this case the FRET efficiency is reduced if aggregation/fusion leads to lipid exchange [155].

To distinguish true vesicle fusion (with mixing of the liposomes' aqueous contents) from simple aggregation, another assay can be performed in which a water-soluble fluorophore is entrapped in one vesicle population (typically ANTS, or Tb^{3+}), while other liposomes contain another molecule which is able to quench (DPX for ANTS) or enhance (DPA for Tb^{3+}) its emission. If the two vesicle populations actually fuse, the entrapped molecules can interact and a change in the fluorescence signal is observed [143]. Recently, a similar assay has been demonstrated to work at the single vesicle level [156]. Obviously, the analysis of this type of experiment is complicated under conditions which allow peptide-induced leakage of the dyes.

Lipid flip-flop

In the toroidal pore model, membrane leakage is coupled to lipid translocation from one leaflet to the other, a phenomenon often referred to as lipid flip-flop [36]. In addition to the need to elucidate the molecular details of the pore formation process, lipid flip-flop (or rather its absence) should also be assessed before performing the peptide translocation assays that rely on membrane asymmetry (see above).

Several assays for lipid flip-flop rely on the differential accessibility to quenchers of lipids in the two membrane leaflets [157]. However, these approaches might be complicated by the presence of peptide-induced pores that would allow the quencher to cross the bilayer. Therefore, they can be used as end-point assays, after stopping peptide-induced leakage by the addition of a protease or of an excess of unlabeled vesicles [20]. However, in our lab another approach is usually preferred [99], in which the ability of bovine serum albumin (BSA) to bind the fluorescent lipid analogue C6-NBD-PC (1-palmitoyl-2-{6-[(7-nitro-2-1,3-benzoxadiazol-4-yl)amino]hexanoyl}-*sn*-glycero-3-phosphocholine) and to quench its fluorescence intensity is exploited [158] (Fig. 1c). Because BSA is usually too big to cross the pores, this assay is not affected by the presence of peptide-induced membrane leakage. In a typical experiment, vesicles labeled with C6-NBD-PC on both layers are incubated with an excess of BSA, so that all external fluorophores are quenched. Then the membrane-active peptide is added, and if it causes lipid flip-flop, labeled lipids which translocate to the outer layer are exposed to BSA and quenched. In this way the flip-flop kinetics can be followed in real time (Fig. 4). Another approach involves FRET between NBD and rhodamine-

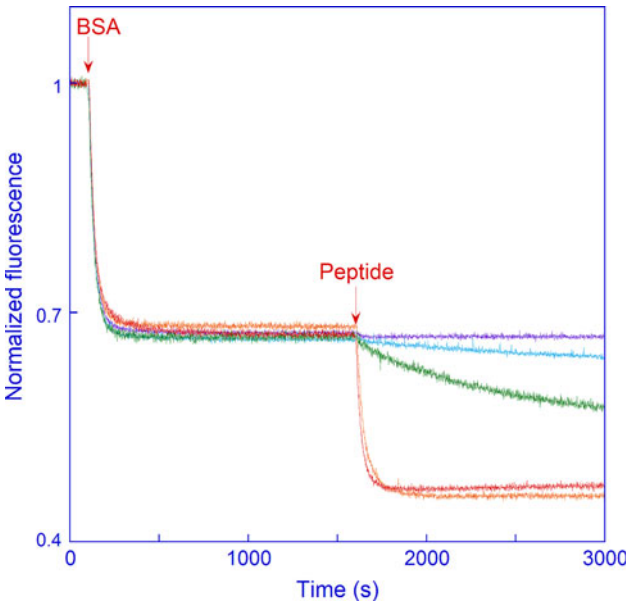

Fig. 4 Kinetics of lipid flip-flop induced by the fluorescent trichogin GA IV analogue F10, as measured by lipid extraction by BSA (previously unpublished data). BSA was added to a suspension of C6-NBD-PC-labeled liposomes (1% molar ratio; total lipid concentration 0.2 mM) at the time indicated by the first *arrow*, in a large excess (final protein concentration 0.2 mM), so that all fluorescent lipids on the external layer were extracted and quenched by the protein. As soon as this process was completed, F10 was added at different concentrations (2.0 μM, *purple*; 4.5 μM, *blue*; 7.0 μM, *green*; 16 μM, *orange*; 25 μM, *red*), at the time indicated by the second *arrow*. As this caused lipid flip-flop, C6-NBD-PC molecules previously located in the internal layer became exposed to the outer leaflet, could be extracted by BSA, and a further decrease in fluorescence intensity was observed. NBD fluorescence was excited at 467 nm and BSA binding was monitored by measuring NBD fluorescence at 522 nm

labeled lipids, which can be initially both on the outer layer, or alternatively one in the outer layer and the other in the inner leaflet. In both cases, FRET efficiency will change if flip-flop takes place [159].

Membrane fluidity and order

In addition to pore formation, many AMPs have been demonstrated to perturb the membrane order and/or dynamics [28]. This membrane disruption can lead to leakage of vesicle contents, but also to malfunction of membrane proteins, in what has been referred to as the sand in a gearbox mechanism [24]. This type of effect can be effectively studied by fluorescence spectroscopy, because the timescale of the excited states and of the typical motions in a lipid bilayer overlap [34].

A typical approach to follow membrane order and dynamics is by measuring the fluorescence anisotropy (steady-state or time-resolved) of a bilayer-embedded probe. DPH is one of the most widely used fluorophores in these experiments [28, 35]. Its strong hydrophobicity

ensures that it partitions strongly in the membrane, and its elongated shape resembles that of a fully extended acyl chain. For this reason the probe orients essentially along the lipid chains, although small populations of other orientations are also present [34]. Furthermore its transition dipole coincides with the long molecular axis and thus the probe motions reflect the overall molecular order experienced by phospholipids in the membrane. We recently applied this approach to show that the AMP Pep-1-K significantly perturbs the bilayer order both below and above the thermotropic phase transition of the membrane [146].

Another approach to sense perturbation in membrane order exploits the unique environmental sensitivity of the spectrum of the dimethylamino naphthalene derivative Laurdan [160]. The emission spectrum of Laurdan reflects the penetration of water molecules into the hydrophobic region of the bilayer as a result of any perturbation of membrane order [160], and it is therefore a probe of membrane packing. For instance, the Laurdan spectrum undergoes a shift of about 50 nm when a lipid bilayer goes from the gel to liquid crystalline phase.

Lateral mobility and domain formation

In addition to the order of the lipid chains along the membrane normal, the association of AMPs to the lipid bilayer can lead to the perturbation of the organization of phospholipids in the plane of the membrane, to the formation of domains, and also to the variation of the lateral lipid diffusional mobility. Indeed, AMPs are often polycationic and their association to the membrane could lead to the sequestration of anionic phospholipids and to lateral separation [23, 24].

If the size of the domains reaches microns, they can be easily observed by optical microscopy, e.g., in GUVs, by employing labeled lipids that co-segregate preferentially in one type of domain [45]. Alternatively, the spectral shifts of Laurdan have been employed to image the presence of domains in different thermotropic phases [45], but this is probably not the type of lateral separation that would be induced by AMP association. Even more importantly, it is likely that the size of the domains that would be induced by AMPs is smaller than the optical resolution, thus making optical microscopic methods inapplicable. In these cases, domains can be sensed by following preferential lipid–lipid interactions. Domain formation will favor these interactions if the two lipids co-segregate in the same domain, whereas it will inhibit it if they segregate in different domains.

The simplest approach of this type employs just one label, i.e., pyrene, taking advantage of its excimers [59] (Fig. 1e). As described in a previous section, excimer formation is influenced both by membrane dynamics and by the local concentration of the labeled lipid, and therefore it is sensitive to domain formation. However, it is important to stress that it is difficult to distinguish between dynamical (i.e., fluidity) and structural (i.e., domain formation) effects with the pyrene experiments alone. DPH anisotropy measurements can help to solve this point by verifying if the peptide causes any change in membrane viscosity. Another approach is based on fluorophore–quencher pairs. Quenching can be caused by short-range quenchers, such as doxyl- or bromine-labeled lipids [161], or by a FRET acceptor [43, 46]. FRET has the advantage that the theoretical efficiency expected for a random donor–acceptor distribution, in the absence of domains, can be calculated. If fluorophore and quencher are attached to the same type of phospholipid, in the case of peptide-induced domain formation they are expected to co-segregate, and the quenching efficiency to increase. By contrast, if the two labels are placed on different lipids that partition in different domains, quenching will decrease in case of domain formation.

Similar experiments can also be performed to verify the lipid selectivity of the peptide. In this case FRET (or quenching) is measured from a peptide-attached fluorophore to a labeled lipid [162]. Preferential interaction with that particular lipid will be demonstrated by a quenching efficiency higher than that expected for a random distribution of acceptors in the plane of the membrane.

MD

MD simulations can provide several important structural and quantitative details on the peptide effects on the membrane.

Regarding the leakage process, the structural picture of the peptide-induced pore that can be obtained from MD simulations can be used to calculate the pore radius, which can then be directly compared with the estimate obtained from liposome-leakage experiments with markers of different sizes. For instance, the program HOLE [163] allows the calculation of the maximal radius of a spherical probe that will fit in the channel at a given depth by means of a Monte Carlo algorithm, and of the ion conductance through the pore. Furthermore, diffusion of ions or other molecules through the channel can be observed directly in the simulations [18, 164, 165]. By applying PMF methods it is possible to determine the free energy profile for the permeation process. Generally, the calculated conductance is in good agreement with the experimental results. In many cases, eventual preferential binding sites for the diffusing ions (associated with the channel selectivity) can be identified [164, 165].

The influence of peptides on lipid flip-flop has been investigated by calculating the PMF profile for the insertion of different lipids in the hydrophobic core of the

bilayer [166]. These simulations showed that the presence of the investigated peptides (WALP23 and KALP23) favors lipid insertion for phosphatidylethanolamine (PE) and phosphatidylglycerol (PG), but not for phosphatidylcholine (PC).

The order of the lipid chains in the membrane can be evaluated from MD simulations by calculating the order parameter (Eq. 4). By comparing simulations of peptide–membrane systems and of free membranes, the perturbing effects of AMPs can be assessed. For instance, melittin produces a decrease in the order parameter of the lipids close to the peptide [167]. The disorder induced by AMPs is usually not confined to the hydrophobic region, but also involves the lipid polar heads. Sengupta et al. [18] in different simulations of melittin in membranes, measured peptide-induced bilayer perturbation by the standard deviation of the coordinates of the phosphate atoms perpendicular to the membrane plane. Even before pore formation, this parameter was influenced by the number of peptides associated to the bilayer. Finally, peptide insertion can perturb the thickness of the membrane, and this is easily visualized in MD simulations. Ulmschneider et al. [168] plotted the local thickness of the bilayer as a function of the radial distance from the peptide as a quantitative estimation of peptide-induced perturbation.

The timescale accessible to CG-MD gives the opportunity to efficiently simulate the process of nanometric domain formation in the presence of AMPs [169]. Simulations carried out with a mixed bilayer formed by PE and PG clearly showed that the Ltc1 peptide increases the size and stability of charged lipid domains. In addition to electrostatic forces, peptide association can also promote domain formation through hydrophobic mismatch in bilayers composed of lipids with different acyl chain lengths [170].

Conclusions

This quick survey of methods, techniques, and experimental approaches is an attempt to give to the reader an idea of the potentialities of fluorescence spectroscopy and MD simulations in the study of the mechanism of action of AMPs. Indeed both approaches already have a key role in this field. However, until now they largely remained two separate worlds. Spectroscopists experimentally obtained a collection of hints about the behavior of peptides in the membrane, and from these incomplete sets of data, they tried to reconstruct a detailed atomic-level picture of the pore formation process. Wimley and Hristova [11] recently compared the researchers in this field to the six blind men in the Indian story, trying to understand what an elephant is by touching only one part of its body. MD simulations, on the other hand, nowadays can directly provide a detailed image of the whole peptide–membrane interaction process. Indeed, several simulations showing AMPs "in action" appeared in the literature [17, 18, 140]. However, this is far from the end of the problem, because these simulations are still affected by sampling limitations, and are always based on severe approximations of the details of the system. Therefore, a direct quantitative comparison with experimental data is essential. The different experimental observables that can be obtained by fluorescence spectroscopy experiments can provide a stringent test of the reliability of the simulation results. MD data, on the other hand, can contribute to clarify the puzzling or misunderstood experimental observations which are often encountered in this field. Therefore, we think that combined studies synergistically employing fluorescence spectroscopy experiments and molecular dynamics simulations have eventually come of age. It is easy to predict that stringent quantitative comparisons between the results obtained with the two approaches, when applied systematically to the same systems, will provide a new level of insight into the mechanism of action of AMPs.

Acknowledgments The authors acknowledge the Italian Ministry of Education, University and Research (PRIN 2008 project), CASPUR, and the Fermi Research Center for financial support.

References

1. Brown KL, Hancock REW (2006) Cationic host defense (antimicrobial) peptides. Curr Opin Immunol 18:24–30
2. Auvynet C, Rosenstein Y (2009) Multifunctional host defense peptides: antimicrobial peptides, the small yet big players in innate and adaptive immunity. FEBS J 276:6497–6508
3. Bechinger B (2009) Rationalizing the membrane interactions of cationic amphipathic antimicrobial peptides by their molecular shape. Curr Opin Colloid Interface Sci 14:349–355
4. Steiner H, Hultmark D, Engström A, Bennich H, Boman HG (1981) Sequence and specificity of two antibacterial proteins involved in insect immunity. Nature 292:246–248
5. Wade D, Boman A, Wxhlin B, Drain CM, Andreu D, Boman HG, Merrifield RB (1990) All-D amino acid-containing channel-forming antibiotic peptides. Proc Natl Acad Sci U S A 87:4761–4765
6. Christensen B, Fink J, Merrifield RB, Mauzerall D (1988) Channel-forming properties of cecropins and related model compounds incorporated into planar lipid membranes. Proc Natl Acad Sci U S A 85:5072–5076
7. Melo MN, Ferre R, Castanho MARB (2009) Antimicrobial peptides: linking partition, activity and high membrane-bound concentrations. Nat Rev Microbiol 7:245–250
8. Zasloff (2002) Antimicrobial peptides of multicellular organisms. Nature 415:389–395
9. Giuliani A, Rinaldi AC (2011) Multimeric peptides and other peptidomimetic approaches. Cell Mol Life Sci. doi:10.1007/s00018-011-0717-3
10. Wimley WC (2010) Describing the mechanism of antimicrobial peptide action with the interfacial activity model. ACS Chem Biol 5:905–917

11. Wimley WC, Hristova K (2011) Antimicrobial peptides: successes, challenges and unanswered questions. J Membr Biol 239:27–34
12. Mueller P (1975) Membrane excitation through voltage-induced aggregation of channel precursors. Ann N Y Acad Sci 264:247–264
13. Qian S, Wang W, Yang L, Huang HW (2008) Structure of the alamethicin pore reconstructed by X-ray diffraction analysis. Biophys J 94:3512–3522
14. Gazit E, Miller IR, Biggin PC, Sansom MS, Shai Y (1996) Structure and orientation of the mammalian antibacterial peptide cecropin P1 within phospholipid membranes. J Mol Biol 258:860–870
15. Matsuzaki K, Murase O, Tokuda H, Funakoshi S, Fujii N, Miyajima K (1994) Orientational and aggregational states of magainin 2 in phospholipid bilayers. Biochemistry 33:3342–3349
16. Ludtke SJ, He K, Heller WT, Harroun TA, Yang L, Huang HW (1996) Membrane pores induced by magainin. Biochemistry 35:13723–13728
17. Leontiadou H, Mark AE, Marrink SJ (2006) Antimicrobial peptides in action. J Am Chem Soc 128:12156–12161
18. Sengupta D, Leontiadou H, Mark AE, Marrink SJ (2008) Toroidal pores formed by antimicrobial peptides show significant disorder. Biochim Biophys Acta 1778:2308–2317
19. Bechinger B, Lohner K (2006) Detergent-like actions of linear amphipathic cationic antimicrobial peptides. Biochim Biophys Acta 1758:1529–1539
20. Orioni B, Bocchinfuso G, Kim JY, Palleschi A, Grande G, Bobone S, Park Y, Kim JI, Hahm KS, Stella L (2009) Membrane perturbation by the antimicrobial peptide PMAP-23: a fluorescence and molecular dynamics study. Biochim Biophys Acta 1788:1523–1533
21. Pokorny A, Birkbeck TH, Almeida PFF (2002) Mechanism and kinetics of δ-lysin interaction with phospholipid vesicles. Biochemistry 41:11044–11056
22. Zhao H, Sood R, Jutila A, Bose S, Fimland G, Nissen-Meyer J, Kinnunen PKJ (2006) Interaction of the antimicrobial peptide pheromone Plantaricin A with model membranes: implications for a novel mechanism of action. Biochim Biophys Acta 1758:1461–1474
23. Epand RM, Epand RF (2011) Bacterial membrane lipids in the action of antimicrobial agents. J Pept Sci 17:298–305
24. Pag U, Oedenkoven M, Sass V, Shai Y, Shamova O, Antcheva N, Tossi A, Sahl HG (2008) Analysis of in vitro activities and modes of action of synthetic antimicrobial peptides derived from an α-helical 'sequence template'. J Antimicrob Chemother 61:341–352
25. Sevcsik E, Pabst G, Jilek A, Lohner K (2007) How lipids influence the mode of action of membrane-active peptides. Biochim Biophys Acta 1768:2586–2595
26. Hong M (2007) Structure, topology, and dynamics of membrane peptides and proteins from solid-state NMR spectroscopy. J Phys Chem B 111:10340–10351
27. Lacapère JJ, Pebay-Peyroula E, Neumann JM, Etchebest C (2007) Determining membrane protein structures: still a challenge! Trends Biochem Sci 32:259–270
28. Bocchinfuso G, Palleschi A, Orioni B, Grande G, Formaggio F, Toniolo C, Park Y, Hahm KS, Stella L (2009) Different mechanisms of action of antimicrobial peptides: insights from fluorescence spectroscopy experiments and molecular dynamics simulations. J Pept Sci 15:550–558
29. Heuck AP, Johnson AE (2002) Pore-forming protein structure analysis in membranes using multiple independent fluorescence techniques. Cell Biochem Biophys 36:89–101
30. Chattopadhyay A, Raghuraman H (2004) Application of fluorescence spectroscopy to membrane protein structure and dynamics. Curr Sci 87:175–180
31. Johnson AE (2005) Fluorescence approaches for determining protein conformations, interactions and mechanisms at membranes. Traffic 6:1078–1092
32. Munishkina LA, Fink AL (2007) Fluorescence as a method to reveal structures and membrane-interactions of amyloidogenic proteins. Biochim Biophys Acta 1768:1862–1885
33. Stella L, Venanzi M, Hahm KS, Formaggio F, Toniolo C, Pispisa B (2008) Shining a light on peptide-lipid interactions. Fluorescence methods in the study of membrane-active peptides. Chem Today 26:44–46
34. Stubb CD, Williams BW (1992) Fluorescence in membranes. In: Lakowicz JR (ed) Topics in fluorescence spectroscopy. Plenum, New York
35. Lentz BR (1993) Use of fluorescent probes to monitor molecular order and motions within liposome bilayers. Chem Phys Lipids 64:99–116
36. Devaux PF, Fellmann P, Herve P (2002) Investigation on lipid asymmetry using lipid probes comparison between spin-labeled lipids and fluorescent lipids. Chem Phys Lipids 116:115–134
37. London E, Ladhokin AS (2002) Measuring the depth of amino acid residues in membrane-inserted peptides by fluorescence quenching. Curr Top Membr 52:89–115
38. Somerharju P (2002) Pyrene-labeled lipids as tools in membrane biophysics and cell biology. Chem Phys Lipids 116:57–74
39. Maier O, Oberle V, Hoekstra D (2002) Fluorescent lipid probes: some properties and applications (a review). Chem Phys Lipids 116:3–18
40. Santos NC, Prieto M, Castanho MARB (2003) Quantifying molecular partition into model systems of biomembranes: an emphasis on optical spectroscopic methods. Biochim Biophys Acta 1612:123–135
41. Henriques ST, Melo MN, Castanho MARB (2007) How to address CPP and AMP translocation? Methods to detect and quantify peptide internalization in vitro and in vivo. Mol Membr Biol 24:173–184
42. Merzlyakov M, Hristova K (2008) Förster resonance energy transfer measurements of transmembrane helix dimerization energetics. Method Enzymol 450:107–127
43. Loura LMS, de Almeida RFM, Silva LC, Prieto M (2009) FRET analysis of domain formation and properties in complex membrane systems. Biochim Biophys Acta 1788:209–224
44. Matos PM, Franquelim HG, Castanho MARB, Santos NC (2010) Quantitative assessment of peptide–lipid interactions. Ubiquitous fluorescence methodologies. Biochim Biophys Acta 1798:1999–2012
45. Bagatolli LA (2006) To see or not to see: lateral organization of biological membranes and fluorescence microscopy. Biochim Biophys Acta 1758:1541–1556
46. Loura LMS, Fernandes F, Prieto M (2010) Membrane microheterogeneity: Förster resonance energy transfer characterization of lateral membrane domains. Eur Biophys J 39:589–607
47. La Rocca P, Biggin PC, Tieleman DP, Sansom MSP (1999) Simulation studies of the interaction of antimicrobial peptides and lipid bilayers. Biochim Biophys Acta 1462:185–200
48. Sansom MS, Shrivastava IH, Bright JN, Tate J, Capener CE, Biggin PC (2002) Potassium channels: structures, models, simulations. Biochim Biophys Acta 1565:294–307
49. Nielsen SO, Lopez CF, Srinivas G, Klein ML (2004) Coarse grain models and the computer simulation of soft materials. J Phys Cond Matt 16:R481–R512
50. Mátyus E, Kandt C, Tieleman DP (2007) Computer simulation of antimicrobial peptides. Curr Med Chem 14:2789–2798

51. Sapay N, Tieleman DP (2008) Molecular dynamics simulation of lipid–protein interactions. Curr Top Membr 60:111–130
52. Bennuna SV, Hoopesb MI, Xingc C, Faller R (2009) Coarse-grained modeling of lipids. Chem Phys Lipids 159:59–66
53. Marrink SJ, de Vries AH, Tieleman DP (2009) Lipids on the move: simulations of membrane pores, domains, stalks and curves. Biochim Biophys Acta 1788:149–168
54. Gurtovenko AA, Anwar J, Vattulainen I (2010) Defect-mediated trafficking across cell membranes: insights from in silico modeling. Chem Rev 110:6077–6103
55. Yu L, Ding JL, Ho B, Feng SS, Wohland T (2008) Investigation of the mechanisms of antimicrobial peptides interacting with membranes by fluorescence correlation spectroscopy. Open Chem Phys J 1:62–79
56. Macháň R, Hof M (2010) Lipid diffusion in planar membranes investigated by fluorescence correlation spectroscopy. Biochim Biophys Acta 1798:1377–1391
57. Rayan G, Guet JE, Taulier N, Pincet F, Urbach W (2010) Recent applications of fluorescence recovery after photobleaching (FRAP) to membrane bio-macromolecules. Sensors 10:5927–5948
58. Lakowicz JR (2006) Principles of fluorescence spectroscopy, 3rd edn. Springer, New York
59. Duportail G, Lianos Q (1996) Fluorescence probing of vesicles using pyrene and pyrene derivatives. In: Rosoff M (ed) Vesicles. Marcel Dekker, New York
60. Clegg RM (2009) Förster resonance energy transfer—FRET what is it, why do it, and how it's done. In: Gadella TWJ (ed) Laboratory techniques in biochemistry and molecular biology (FRET and FLIM techniques). Elsevier, Amsterdam
61. Yengo CM, Berger CL (2010) Fluorescence anisotropy and resonance energy transfer: powerful tools for measuring real time protein dynamics in a physiological environment. Curr Opin Pharmacol 10:731–737
62. Ferreira ST, Stella L, Gratton E (1994) Conformational dynamics of bovine Cu, Zn superoxide dismutase revealed by time-resolved fluorescence spectroscopy of the single tyrosine residue. Biophys J 66:1185–1196
63. Stella L, Venanzi M, Carafa M, Maccaroni E, Straccamore ME, Zanotti G, Palleschi A, Pispisa B (2002) Structural features of model glycopeptides in solution and in membrane phase. A spectroscopic and molecular mechanics investigation. Biopolymers 64:44–56
64. Stella L, Mazzuca C, Venanzi M, Palleschi A, Didonè M, Formaggio F, Toniolo C, Pispisa B (2004) Aggregation and water-membrane partition as major determinants of the activity of the antibiotic peptide trichogin GA IV. Biophys J 86:936–945
65. Epand RM, Epand RF (2003) Liposomes as models for antimicrobial peptides. Methods Enzymol 372:124–133
66. Ladokhin AS, Fernandez-Vidal M, White SH (2010) CD spectroscopy of peptides and proteins bound to large unilamellar vesicles. J Membr Biol 236:247–253
67. Walde P, Cosentino K, Engel H, Stano P (2010) Giant vesicles: preparations and applications. Chem Biochem 11:848–865
68. Méléard P, Bagatolli LA, Pott T (2009) Giant unilamellar vesicle electroformation from lipid mixtures to native membranes under physiological conditions. Methods Enzymol 465:161–176
69. Smit B, Hilbers PAJ, Esselink K, Rupert LAM, van Os NM, Schlijper AG (1990) Computer-simulations of a water oil interface in the presence of micelles. Nature 348:624–625
70. Drouffe J, Maggs A, Leibler S (1991) Computer simulations of self-assembled membranes. Science 254:1353–1356
71. Marrink SJ, de Vries AH, Mark AE (2004) Coarse grained model for semiquantitative lipid simulations. J Phys Chem B 108:750–760
72. Lyubartsev AP (2005) Multiscale modeling of lipids and lipid bilayers. Eur Biophys J 35:53–61
73. Izvekov S, Voth GA (2005) A multiscale coarse-graining method for biomolecular systems. J Phys Chem B 109:2469–2473
74. Elezgaray J, Laguerre M (2006) A systematic method to derive force fields for coarsegrained simulations of phospholipids. Comp Phys Comm 175:264–268
75. Bond PJ, Holyoake J, Ivetac A, Khalid S, Sansom MSP (2007) Coarse-grained molecular dynamics simulations of membrane proteins and peptides. J Struct Biol 157:593–605
76. Marrink SJ, Risselada J, Yefimov S, Tieleman DP, de Vries AH (2007) The MARTINI force field: coarse grained model for biomolecular simulations. J Phys Chem B 111:7812–7824
77. Khalfa A, Treptow W, Maigret B, Tarek M (2009) Self assembly of peptides near or within membranes using coarse grained MD simulations. Chem Phys 358:161–170
78. Monticelli L, Tieleman DP, Fuchs PFJ (2010) Interpretation of 2H-NMR experiments on the orientation of the transmembrane helix WALP23 by computer simulations. Biophys J 99:1455–1464
79. Kirkwood JG (1935) Statistical mechanics of fluid mixtures. J Chem Phys 3:300–313
80. Torrie GM, Valleau JP (1977) Non physical sampling distributions in Monte Carlo free energy estimation—umbrella sampling. J Comput Phys 23:187–199
81. Kumarv S, Bouzida D, Swendsen R, Kollman PA, Rosenberg JM (1992) The weighted histogram analysis method for free-energy calculations on biomolecules. 1. The method. J Comput Chem 13:1011–1021
82. Roux B (1995) The calculation of the potential of mean force using computer simulations. Comput Phys Commun 91:275–282
83. Wee CL, Ulmschneider MB, Sansom MSP (2010) Membrane/toxin interaction energetics via serial multiscale molecular dynamics simulations. J Chem Theory Comput 6:966–976
84. Yesylevskyy S, Marrink SJ, Mark AE (2009) Alternative mechanisms for the interaction of the cell-penetrating peptides penetratin and the TAT peptide with lipid bilayers. Biophys J 97:40–49
85. Bond PJ, Parton DL, Clark JF, Sansom MSP (2008) Coarse-grained simulations of the membrane-active antimicrobial peptide maculatin 1.1. Biophys J 95:3802–3815
86. Khandelia H, Kaznessis YN (2005) Molecular dynamics simulations of the helical antimicrobial peptide ovispirin-1 in zwitterionic dodecylphoshocholine micelles. J Phys Chem B 109:12990–12996
87. Langham AA, Khandelia H, Kaznessis YN (2006) How can a β-sheet peptide be both a potent antimicrobial and harmfully toxic? Molecular dynamics simulations of protegrin-1 in micelles. Biopolymers 84:219–231
88. White SH, Wimley WC, Ladokhin AS, Hristova K (1998) Protein folding in membranes: determining energetics of peptide-bilayer interactions. Methods Enzymol 295:62–87
89. Eftink R (2000) Use of fluorescence spectroscopy as thermodynamics tool. Methods Enzymol 323:459–473
90. Seelig J (2004) Thermodynamics of lipid–peptide interactions. Biochim Biophys Acta 1666:40–50
91. Schwarz G (2000) A universal thermodynamic approach to analyze biomolecular binding experiments. Biophys Chem 86:119–129
92. Rodinger T, Pomès R (2005) Enhancing the accuracy the efficiency and the scope of free energy simulations. Curr Opin Struct Biol 15:164–170
93. Monticelli LS, Kandasamy K, Periole X, Larson RG, Tieleman DP, Marrink SJ (2008) The MARTINI coarse grained force field: extension to proteins. J Chem Theory Comput 4:819–834

94. Stella L, Burattini M, Mazzuca C, Palleschi A, Venanzi M, Coin I, Peggion C, Formaggio F, Toniolo C, Pispisa B (2007) Alamethicin interaction with lipid membranes: a spectroscopic study on synthetic analogues. Chem Biodivers 4:1299–1312
95. Eftink MR, Ghiron CA (1981) Fluorescence quenching studies with proteins. Anal Biochem 114:199–227
96. Pispisa B, Palleschi A, Stella L, Venanzi M, Toniolo C (1998) A nitroxide derivative as a probe for conformational studies of short linear peptides in solution. A spectroscopic and molecular mechanics investigation. J Phys Chem B 102:7890–7898
97. Caputo GA, London E (2003) Using a novel dual fluorescence quenching assay for measurement of tryptophan depth within lipid bilayers to determine hydrophobic alpha-helix locations within membranes. Biochemistry 42:3265–3274
98. Menger FM, Keiper JS, Caran KL (2002) Depth profiling with giant vesicle membranes. J Am Chem Soc 124:11842–11843
99. Mazzuca C, Stella L, Venanzi M, Formaggio F, Toniolo C, Pispisa B (2005) Mechanism of membrane activity of the antibiotic trichogin GA IV: a two-state transition controlled by peptide concentration. Biophys J 88:3411–3421
100. Ciobanasu C, Siebrassea JP, Kubitscheck U (2010) Cell-penetrating HIV1 TAT peptides can generate pores in model membranes. Biophys J 99:153–162
101. Szeto HH, Schiller PW, Zhao K, Luo G (2005) Fluorescent dyes alter intracellular targeting and function of cell-penetrating tetrapeptides. FASEB J 19:119–120
102. Bárány-Wallje E, Keller S, Serowy S, Geibel S, Pohl P, Bienert M, Dathe M (2005) A critical reassessment of penetratin translocation across lipid membranes. Biophys J 89:2513–2521
103. Matsuzaki K, Murase O, Fujii N, Miyajima K (1995) Translocation of a channel forming antimicrobial peptide, magainin 2, across lipid bilayers by forming a pore. Biochemistry 34:6521–6526
104. Wimley WC, White SH (2000) Determining the membrane topology of peptides by fluorescence quenching. Biochemistry 39:161–170
105. Fattal E, Nir S, Parente RA, Szoka FC Jr (1994) Pore-forming peptides induce rapid phospholipid flip-flop in membranes. Biochemistry 33:6721–6731
106. Keller S, Böthe M, Bienert M, Margitta Dathe M, Blume A (2007) A simple fluorescence-spectroscopic membrane translocation assay. ChemBioChem 8:546–552
107. Babakhani A, Gorfe AA, Gullingsrud J, Kim JE, McCammon JA (2007) Peptide insertion, positioning, and stabilization in a membrane: insight from an all-atom molecular dynamics simulation. Biopolymers 85:490–497
108. Babakhani A, Gorfe AA, Kim JE, McCammon JA (2008) Thermodynamics of peptide insertion and aggregation in a lipid bilayer. J Phys Chem B 112:10528–10534
109. Bond PJ, Wee CL, Sansom MSP (2008) Coarse-grained molecular dynamics simulations of the energetics of helix insertion into a lipid bilayer. Biochemistry 47:11321–11331
110. Gkeka P, Sarkisov L (2010) Interaction of phospholipid bilayers with several classes of amphiphilic α-helical peptides: insights from coarse-grained molecular dynamics simulations. J Phys Chem B 114:826–839
111. Goetz R, Gompper G, Lipowsky R (1999) Mobility and elasticity of self-assembled membranes. Phys Rev Lett 82:221–224
112. Venturoli M, Smit B (1999) Simulating the self-assembly of model membranes. Phys Chem Comm 2:45–49
113. Marrink SJ, Lindahl E, Edholm O, Mark AE (2001) Simulation of the spontaneous aggregation of phospholipids into bilayers. J Am Chem Soc 123:8638–8639
114. de Vries AH, Mark AE, Marrink SJ (2004) The binary mixing behavior of phospholipids in a bilayer: a molecular dynamics study. J Phys Chem B 108:2454–2463
115. Bond PJ, Sansom MSP (2006) Insertion and assembly of membrane proteins via simulation. J Am Chem Soc 128:2697–2704
116. Esteban-Martin S, Salgado J (2007) Self-assembling of peptide/membrane complexes by atomistic molecular dynamics simulations. Biophys J 92:903–912
117. Bond PJ, Sansom MSP (2007) Bilayer deformation by the Kv channel voltage sensor domain revealed by self-assembly simulations. Proc Natl Acad Sci U S A 104:2631–2636
118. Scott KA, Bond PJ, Ivetac A, Chetwynd AP, Khalid S, Sansom MSP (2008) Coarse-grained MD simulations of membrane protein/bilayer self assembly. Structure 16:621–630
119. Sansom MSP, Scott KA, Bond PJ (2008) Coarse-grained simulation: a high throughput computational approach to membrane proteins. Biochem Soc Trans 36:27–32
120. Gurtovenko AA, Vattulainen I (2007) Molecular mechanism for lipid flip-flops. J Phys Chem B 111:13554–13559
121. Gatto E, Mazzuca C, Stella L, Venanzi M, Toniolo C, Pispisa B (2006) Effect of peptide lipidation on membrane perturbing activity: a comparative study on two trichogin analogues. J Phys Chem B 110:22813–22818
122. Tieleman DP, Hess B, Sansom MSP (2002) Analysis and evaluation of channel models: simulations of alamethicin. Biophys J 83:2393–2407
123. Pispisa B, Stella L, Mazzuca C, Venanzi M (2006) Trichogin topology and activity in model membranes as determined by fluorescence spectroscopy. Rev Fluoresc 2006:47–70
124. Sparr E, Ash WL, Nazarov PV, Rijkers DTS, Hemminga MAD, Tieleman P, Killian JA (2005) Self-association of transmembrane α-helices in model membranes: importance of helix orientation and role of hydrophobic mismatch. J Biol Chem 280:39324–39331
125. Fung B, Stryer L (1978) Surface density measurements in membranes by fluorescence resonance energy transfer. Biochemistry 17:5241–5248
126. Fernandes F, Loura LM, Prieto M, Koehorst R, Spruijt RB, Hemminga MA (2003) Dependence of M13 major coat protein oligomerization and lateral segregation on bilayer composition. Biophys J 85:2430–2441
127. Caflisch A (2006) Computational models for the prediction of polypeptide aggregation propensity. Curr Opin Chem Biol 10:437–444
128. Colombo G, Soto P, Gazit E (2007) Peptide self-assembly at the nanoscale: a challenging target for computational and experimental biotechnology. Trends Biotech 25:211–218
129. Henin J, Pohorille A, Chipot C (2005) Insights into the recognition and association of transmembrane α-helices. The free energy of α-helix dimerization in glycophorin A. J Am Chem Soc 127:8478–8484
130. Bu L, Im W, Brooks CL (2007) Membrane assembly of simple helix homo-oligomers studied via molecular dynamics simulations. Biophys J 92:854–863
131. Khalfa A, Tarek M (2010) On the antibacterial action of cyclic peptides: insights from coarse-grained MD simulations. J Phys Chem 114:2676–2684
132. Herrera AI, Al-Rawi A, Cook GA, Gao J, Iwamoto T, Prakash O, Tomich JM, Chen J (2010) Structural characterization of two pore-forming peptides: consequences of introducing a C-terminal tryptophan proteins 78:2238–2250
133. Nguyen THT, Rao NZ, Schroeder WM, Moore PB (2010) Coarse-grained molecular dynamics of tetrameric transmembrane peptide bundles within a lipid bilayer. Chem Phys Lipids 163:530–537
134. Jo S, Lim JB, Klauda JB, Im W (2009) CHARMM-GUI membrane builder for mixed bilayers and its application to yeast membranes. Biophys J 97:50–58

135. Kandt C, Ash WL, Tieleman DP (2007) Setting up and running molecular dynamics simulations of membrane proteins. Methods 41:475–488
136. Carpenter T, Bond PJ, Khalid S, Sansom MSP (2008) Self-assembly of a simple membrane protein: coarse-grained molecular dynamics simulations of the influenza M2 channel. Biophys J 2008:3790–3801
137. Thøgersen L, Schiøtt B, Vosegaard T, Nielsen NC, Tajkhorshid E (2008) Peptide aggregation and pore formation in a lipid bilayer; a combined coarse grained and all atom molecular dynamics study. Biophys J 95:4337–4347
138. Psachoulia E, Marshall DP, Sansom MSP (2010) Molecular dynamics simulations of the dimerization of transmembrane α-helices. Acc Chem Res 43:388–396
139. Rzepiela AJ, Schäfer LV, Goga N, Risselada HJ, De Vries AH, Marrink SJ (2010) Reconstruction of atomistic details from coarse-grained structures. J Comput Chem 31:1333–1343
140. Rzepiela AJ, Sengupta D, Goga N, Marrink SJ (2010) Membrane poration by antimicrobial peptides combining atomistic and coarse-grained descriptions. Faraday Discuss 144:431–443
141. Mazzuca C, Orioni B, Coletta M, Formaggio F, Toniolo C, Maulucci G, De Spirito M, Pispisa B, Venanzi M, Stella L (2010) Fluctuations and the rate-limiting step of peptide-induced membrane leakage. Biophys J 99:1791–1800
142. Ladokhin AS, Wimley WC, White SH (1995) Leakage of membrane vesicle contents: determination of mechanism using fluorescence requenching. Biophys J 69:1964–1971
143. Wilschut J, Papahadjopoulos D (1979) Ca^{2+}-induced fusion of phospholipid vesicles monitored by mixing of aqueous contents. Nature 281:690–692
144. Ladokhin AS, Selsted ME, White SH (1997) Sizing membrane pores in lipid vesicles by leakage of co-encapsulated markers: pore formation by melittin. Biophys J 72:1762–1766
145. Ostolaza H, Bartolomé B, Ortiz de Zárate I, de la Cruz F, Goñi FM (1993) Release of lipid vesicle contents by the bacterial protein toxin α-haemolysin. Biochim Biophys Acta 1147:81–88
146. Bobone S, Piazzon A, Orioni B, Pedersen JZ, Nan YH, Hahm KS, Shin SY, Stella L (2011) The thin line between cell-penetrating and antimicrobial peptides: the case of Pep-1 and Pep-1-K. J Pept Sci 17:335–341
147. Minta A, Tsien RY (1989) Fluorescent indicators for cytosolic sodium. J Biol Chem 264:19449–19457
148. Tamba U, Yamazaki M (2005) Single giant unilamellar vesicle method reveals effect of antimicrobial peptide magainin 2 on membrane permeability. Biochemistry 44:15823–15833
149. Tamba Y, Ariyama H, Levadny V, Yamazaki M (2010) Kinetic pathway of antimicrobial peptide magainin 2-induced pore formation in lipid membranes. J Phys Chem B 114:12018–12026
150. Fuertes G, García-Sáez AJ, Esteban-Martín S, Giménez D, Sánchez-Muñoz OL, Schwille P, Salgado J (2010) Pores formed by Baxα5 relax to a smaller size and keep at equilibrium. Biophys J 99:2917–2925
151. Apellániz B, Nieva JL, Schwille P, García-Sáez AJ (2010) All-or-none versus graded: single-vesicle analysis reveals lipid composition effects on membrane permeabilization. Biophys J 99:3619–3628
152. Rausch JM, Marks JR, Rathinakumar R, Wimley WC (2007) Beta-sheet pore-forming peptides selected from a rational combinatorial library: mechanism of pore formation in lipid vesicles and activity in biological membranes. Biochemistry 46:12124–12139
153. Marquette A, Lorber B, Bechinger B (2010) Reversible liposome association induced by LAH4: a peptide with potent antimicrobial and nucleic acid transfection activities. Biophys J 98:2544–2553
154. Loura LMS, Prieto M (2009) Characterization of peptide-induced morphological alterations in membranes by fluorescence resonance energy transfer. Protein Pept Lett 16:726–735
155. Struck DK, Hoekstra D, Pagano RE (1981) Use of resonance energy transfer to monitor membrane fusion. Biochemistry 20:4093–4099
156. Diao J, Su Z, Ishitsuka Y, Lu B, Lee KS, Lai Y, Shin YK, Ha T (2010) A single-vesicle content mixing assay for SNARE-mediated membrane fusion. Nat Comm 1:54
157. Matsuzaki M, Murase O, Fujii N, Miyajima K (1996) An antimicrobial peptide, magainin 2, induced rapid flip-flop of phospholipids coupled with pore formation and peptide translocation. Biochemistry 35:11361–11368
158. Marx U, Lassman G, Holzütter HG, Wüstner D, Müller P, Höhlig A, Kubelt J, Herrmann A (2000) Rapid flip-flop of phospholipids in endoplasmic reticulum membranes studied by a stopped-flow approach. Biophys J 78:2628–2640
159. Wolf DE, Winiski AP, Ting AE, Bocian KM, Pagano RE (1992) Determination of the transbilayer distribution of fluorescent lipid analogues by nonradiative fluorescence resonance energy transfer. Biochemistry 31:2865–2873
160. Parasassi T, Krasnowska EK, Bagatolli L, Gratton E (1998) Laurdan and Prodan as polarity-sensitive fluorescent membrane probes. J Fluoresc 8:365–373
161. London E (2002) Insights into lipid raft structure and formation from experiments in model membranes. Curr Opin Struct Biol 12:480–486
162. Loura LMS, Prieto M, Fernandes F (2010) Quantification of protein-lipid selectivity using FRET. Eur Biophys J 39:565–578
163. Smart OS, Neduvelil JG, Wang X, Wallace BA, Sansom MSP (1996) HOLE: a program for the analysis of the pore dimensions of ion channel structural models. J Mol Graph 14:354–360
164. Allen TW, Andersen OS, Roux B (2006) Ion permeation through a narrow channel: using gramicidin to ascertain all-atom molecular dynamics potential of mean force, methodology and biomolecular force fields. Biophys J 90:3447–3468
165. Kandasamy SK, Larson RG (2006) Cation and anion transport through hydrophilic pores in lipid bilayers. J Chem Phys 125:074901
166. Sapay N, Bennet WFD, Tieleman DP (2010) Molecular simulations of lipid flip-flop in the presence of model transmembrane helices. Biochemistry 49:7665–7673
167. Bachar M, Becker OM (2000) Protein-induced membrane disorder: a molecular dynamics study of melittin in a dipalmitoylphosphatidylcholine bilayer. Biophys J 78:1359–1375
168. Ulmschneider MB, Doux JPF, Killian JA, Smith JC, Ulmschneider JP (2010) Mechanism and kinetics of peptide partitioning into membranes from all-atom simulations of thermostable peptides. J Am Chem Soc 132:3452–3460
169. Polyansky AA, Ramaswamy R, Volynsky PE, Sbalzarini IF, Marrink SJ, Efremov RG (2010) Antimicrobial peptides induce growth of phosphatidylglycerol domains in a model bacterial membrane. J Phys Chem Lett 1:3108–3111
170. Klingelhoefer JW, Carpenter T, Sansom MSP (2009) Peptide nanopores and lipid bilayers: interactions by coarse-grained molecular-dynamics simulations. Biophys J 96:3519–3528